Molecular Cell
Article

A Ubiquitin Ligase-Associated Chaperone Holdase Maintains Polypeptides in Soluble States for Proteasome Degradation

Qiuyan Wang,[1,3] Yanfen Liu,[1,3] Nia Soetandyo,[1] Kheewoong Baek,[1] Ramanujan Hegde,[2] and Yihong Ye[1,*]
[1]Laboratory of Molecular Biology, National Institute of Diabetes and Digestive and Kidney Diseases
[2]Cell Biology and Metabolism Program, National Institute of Child Health and Human Development
National Institutes of Health, Bethesda, MD 20892, USA
[3]These authors contributed equally to this work
*Correspondence: yihongy@mail.nih.gov
DOI 10.1016/j.molcel.2011.05.010

SUMMARY

Endoplasmic reticulum-associated degradation (ERAD) employs membrane-bound ubiquitin ligases and the translocation-driving ATPase p97 to retrotranslocate misfolded proteins for proteasomal degradation. How retrotranslocated polypeptides bearing exposed hydrophobic motifs or transmembrane domains (TMDs) avoid aggregation before reaching the proteasome is unclear. Here we identify a ubiquitin ligase-associated multiprotein complex comprising Bag6, Ubl4A, and Trc35, which chaperones retrotranslocated polypeptides en route to the proteasome to improve ERAD efficiency. In vitro, Bag6, the central component of the complex, contains a chaperone-like activity capable of maintaining an aggregation-prone substrate in an unfolded yet soluble state. The physiological importance of this holdase activity is underscored by observations that ERAD substrates accumulate in detergent-insoluble aggregates in cells depleted of Bag6, or of Trc35, a cofactor that keeps Bag6 outside the nucleus for engagement in ERAD. Our results reveal a ubiquitin ligase-associated holdase that maintains polypeptide solubility to enhance protein quality control in mammalian cells.

INTRODUCTION

In eukaryotic cells, thousands of secretory and membrane proteins are translocated into the lumen of the endoplasmic reticulum (ER) or integrated into the ER membrane before being delivered to their final destinations. Despite the presence of a large number of ER chaperones that assist nascent polypeptides in folding and assembly, protein misfolding occurs frequently. To deal with this problem, eukaryotic cells have evolved a protein quality control mechanism, through which misfolded ER proteins are selectively retained and subsequently retrotranslocated into the cytosol. Retrotranslocated polypeptides are degraded by the ubiquitin proteasome system (Hirsch et al., 2009; Vembar and Brodsky, 2008). This garbage disposal process, named ER-associated degradation (ERAD) or retrotranslocation, alleviates ER stress to improve cell vitality (Ron and Walter, 2007). Interestingly, certain pathogens can co-opt the ERAD pathway to dispose of native proteins essential for immune defense. For example, the human cytomegalovirus (HCMV) genome encodes two proteins, US2 and US11, each of which can downregulate newly synthesized major histocompatibility complex (MHC) class I heavy chain (HC) at the ER membrane (Lilley and Ploegh, 2005). These viral proteins can bind HC and target it to membrane dislocation complexes for retrotranslocation and degradation (Lilley and Ploegh, 2004; Ye et al., 2004).

ERAD employs a variety of chaperones and lectins such as BiP, Os9, EDEM, and PDI, which selectively recognize terminally misfolded proteins carrying immature glycans, exposed hydrophobic regions, or unpaired cysteine residues (Buchberger et al., 2011). Misfolded polypeptides are then moved across the ER membrane to enter into the cytosol. The mechanisms underlying protein retrotranslocation are unclear, but existing evidence suggests that retrotranslocation of distinct cohorts of substrates is mediated by different membrane complexes. These complexes often contain one or more multispanning transmembrane ubiquitin ligases (E3) and the p97 ATPase. Although not yet proven, the dislocation complexes likely form a few protein conducting channels through which misfolded proteins exit the ER. Once reaching the cytosolic side of the membrane, substrates are polyubiquitinated by the E3s. In mammalian cells, several ERAD-dedicated E3s including Hrd1, gp78, TEB4, Kf-1, RMA1, and TRC8 have been identified (Hirsch et al., 2009). Ubiquitinated ERAD substrates are dislocated from the membrane by p97 and its associated cofactors (Bays et al., 2001; Jarosch et al., 2002; Rabinovich et al., 2002; Ye et al., 2001). p97 subsequently hands substrates off to the proteasome with the assistance of several shuttling factors.

Several lines of evidence indicate that the putative retrotranslocons cannot accommodate tightly folded polypeptides or protein aggregates, possibly due to size constraints (Bhamidipati et al., 2005; Nishikawa et al., 2001; Okuda-Shimizu and Hendershot, 2007; Soetandyo et al., 2010). First, fusion of a tightly folded domain to the model ERAD substrate CPY* abolishes its

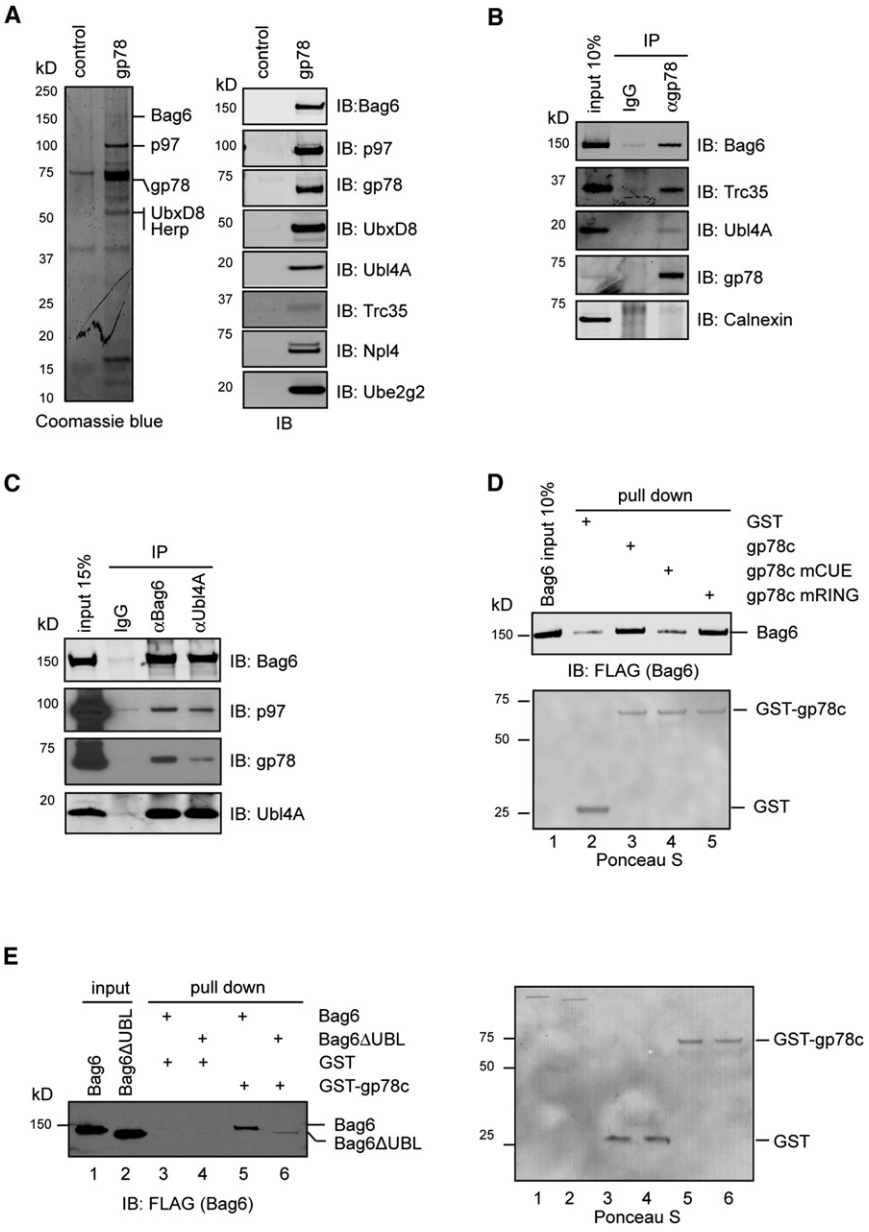

Figure 1. The Bag6 Complex Interacts with the gp78-p97 Retrotranslocation Complex

(A) Identification of the Bag6 complex as an interaction partner of gp78. Cell extracts from 293T cells transfected with FLAG-tagged gp78 or a control plasmid were subject to immunoprecipitation (IP) with FLAG antibody. IB, immunoblotting.

(B and C) Endogenous interactions between the Bag6 and the gp78-p97 complexes. 293T cell extract was subject to IP analyses using the indicated antibodies.

(D) Bag6 directly binds the cytosolic domain of gp78 via the CUE domain. The indicated GST-tagged proteins were immobilized on glutathione beads and incubated with purified Bag6.

(E) The UBL domain in Bag6 is required for gp78 interaction. Purified Bag6 or a Bag6 variant lacking UBL was incubated with glutathione beads containing GST-gp78c or GST. The right panel shows the Ponceau S-stained membrane used for immunoblotting (left panel). See also Figure S1.

retrotranslocation and degradation (Bhamidipati et al., 2005). Second, for unassembled TCRα chain, two intramembrane charged residues prevent interchain disulfide formation, which facilitates TCRα degradation by maintaining it in a retrotranslocation-competent monomeric state (Soetandyo et al., 2010). Moreover, the retrotranslocation of nonsecreted κ-LC requires the conversion of a partially oxidized precursor into a reduced monomer (Okuda-Shimizu and Hendershot, 2007). Lastly, many ER chaperones with unfolding activities have been identified to mediate retrotranslocation (Bernardi et al., 2008; Lee et al., 2010; Nishikawa et al., 2001; Ushioda et al., 2008). Together, these findings suggest that ERAD substrates are most likely retrotranslocated across the membrane in unfolded forms. Thus, dislocated polypeptides are expected to bear exposed hydrophobic motifs or TMDs prone to aggregation in the aqueous cytosolic environment. These hydrophobic motifs need to be properly shielded before substrates are safely targeted to the proteasome. Otherwise, substrate aggregation could prematurely terminate the degradation process. Here, we report a chaperone holdase complex that maintains the solubility of retrotranslocated polypeptides to promote ER protein quality control in mammalian cells.

RESULTS

The Bag6 Complex Interacts with ERAD E3s

To identify factors that facilitate ERAD, we expressed in 293T cells the ER-associated ubiquitin ligase gp78, which is responsible for the degradation of many ERAD substrates (Fang et al., 2001; Shen et al., 2006; Song et al., 2005). We performed affinity purification to isolate gp78 and its associated proteins. The Coomassie-stained gel revealed several gp78-associated proteins (Figure 1A). Peptide sequencing by mass spectrometry and immunoblotting identified many of them as known ERAD factors, including p97, Npl4, Ube2g2, UbxD8, and Herp (Alexandru et al., 2008; Chen et al., 2006; Li et al., 2007; Schulze et al., 2005; Zhong et al., 2004). Interestingly, an ~150 kD protein was identified as Bag6, a gp78 partner with no previously documented function in ERAD (see Figure S1A available online).

Bag6 was recently identified as the central component of a stable three-protein complex that also contains Ubl4A and Trc35, which promotes membrane targeting of ER tail-anchored (TA) proteins (Leznicki et al., 2010; Mariappan et al., 2010). Using

Bag6-, Ubl4A-, and Trc35-specific antibodies, we confirmed that these proteins all associated with gp78-FLAG (Figure 1A). Moreover, each component of the Bag6 complex could be coprecipitated with endogenous gp78 by a gp78 antibody, whereas the ER lectin calnexin failed to bind gp78 (Figure 1B). Reciprocal immunoprecipitation showed that both Bag6 and Ubl4A antibodies precipitated the Bag6 complex together with endogenous gp78 and p97 (Figure 1C). These results demonstrate an interaction between the Bag6 complex and the gp78-p97 retrotranslocation complex in the cell.

To further define the interaction between the Bag6 complex and gp78, we performed a series of pull-down experiments using purified proteins. A direct interaction between gp78 and Bag6 could be established using full-length Bag6 and a GST-tagged cytosolic domain of gp78 (gp78c) (Figure 1D, lane 3 versus lane 2). A ligase-defective gp78c mutant (mRING) also interacted with Bag6 (lane 5). However, a gp78c CUE mutant defective in ubiquitin recognition (Chen et al., 2006) failed to bind Bag6 (lane 4). On the Bag6 side, deletion of its N-terminal ubiquitin-like (UBL) domain dramatically impaired the interaction with gp78, albeit not completely abolishing it (Figure 1E, lane 6 versus lane 5; Figure S1B). Thus, Bag6 appears to have two binding sites for gp78, with the one localized in the UBL domain being recognized by the gp78 CUE domain. Hrd1, another ERAD-specific E3, also interacted with Bag6 (Figure S1C). Hrd1 does not contain a CUE domain. Accordingly, the Hrd1-Bag6 interaction was independent of the Bag6 UBL domain (Figure S1D).

Trc35 Retains Bag6 in the Cytosol

We next characterized the subcellular localization of the Bag6 complex. Subcellular fractionation and immunoblotting showed that the Bag6 complex was present in both cytosol and an ER-containing membrane fraction (Figure S2). This observation was intriguing because Bag6 was predicted to be a nuclear protein with a nuclear localization signal (NLS) (Desmots et al., 2005; Minami et al., 2010; Nguyen et al., 2008). We postulated that a cytosolically localized interacting partner might maintain a cytosolic pool of Bag6, which could associate with ERAD-specific ubiquitin ligases. Indeed, we found by a series of immunostaining experiments that Trc35, but not Ubl4A, could mask Bag6 NLS to retain it in the cytoplasm. Our data showed that endogenous Bag6 was present in both nucleus and cytoplasm (Figure 2A, panels 1–3), whereas overexpressed Bag6 was mostly localized to the nucleus (Figure 2B, panel 1), likely because of insufficient Trc35. Consistent with this interpretation, overexpression of Trc35, which was a cytosolically localized protein by itself (Figure 2B, panel 2), almost completely eliminated the nuclear localization of both endogenous and overexpressed Bag6, resulting in a cytosolic staining pattern for Bag6 (Figure 2A, panels 4–6; Figure 2B, panels 7–9). By contrast, Ubl4A itself was localized in both cytosol and nucleus (Figure 2B, panel 3), and coexpression of Bag6 with Ubl4A enriched both proteins in the nucleus (Figure 2B, panels 4–6). Bag6 apparently can carry Ubl4A into the nucleus when endogenous Trc35 is insufficient to keep overexpressed Bag6 in the cytosol.

We also examined the effect of Trc35 knockdown on Bag6 localization. Immunostaining with a Bag6 antibody showed that in control cells Bag6 was localized both in the cytosol and in the nucleus (Figure 2C, panels 1 and 2). Confocal microscopy analyses showed on average no significant change in fluorescence intensity across the nuclear envelop boundary (Figures 2C and 2D). In contrast, ~60% of the cells treated with a Trc35 shRNA construct displayed an apparent enrichment of Bag6 in the nucleus (Figure 2C, panels 3 and 4; Figure 2D). These data further support the notion that Trc35 is required for maintaining a cytosolic pool of Bag6.

The Bag6 Complex Interacts with TCRα

To test the possible involvement of the Bag6 complex in ERAD, we assessed its association with TCRα, a model ERAD substrate whose degradation requires gp78 (Chen et al., 2006). Because substrate binding to ERAD machinery factors occurs in a dynamic fashion, we treated cells stably expressing YFP-tagged TCRα with the proteasome inhibitor MG132 to halt the constant flow of substrate to the proteasome. As expected, when TCRα was immunoprecipitated, several known ERAD factors including p97, gp78, and the proteasome could be detected in the precipitated TCRα complex in a MG132-dependent manner (Figure S3A). The Bag6 complex also interacted with TCRα in a similar manner (Figure 3A; Figure S3A). The interaction of Bag6 with TCRα must occur in the cell because a similar coimmunoprecipitation experiment performed with MG132-treated cell extract containing exogenously added recombinant Bag6 failed to detect significant interactions between TCRα and the exogenous Bag6 (Figure S3B). Interestingly, when p97 level was knocked down, interactions of TCRα with Bag6 and the proteasome were reduced (Figure 3B), indicating that like the proteasome, Bag6 encountered TCRα following its retrotranslocation by p97. The Bag6-TCRα complex was stable in both NP40 and RIPA lysis buffer, although the latter contained the strong detergent sodium dodecyl sulfate (SDS), which disrupted protein interactions, as revealed by the significant loss of TCRα interaction with p97 (Figure 3C). Together, these results indicate that Bag6 may directly interact with TCRα during retrotranslocation in the cell.

The Bag6 Complex Facilitates ERAD

To determine whether the Bag6 complex functions in ERAD, we first tested whether the degradation of TCRα was impaired in Bag6 knockdown cells. When the level of TCRα was measured by flow cytometry and immunoblotting, it was indeed increased in Bag6 knockdown cell (Figure 4A). Knockdown of Bag6 also increased the steady state level of another ERAD substrate CD4 in cells expressing the HIV protein Vpu (Figure 4B) as well as a TCRα variant lacking TMD (see below). By contrast, the degradation of a cytosolic proteasome substrate (Ub-V-GFP) was largely unaffected by Bag6 knockdown (Figure 4C).

When cycloheximide chase was used to compare the half-life of TCRα in control and Bag6 knockdown cells, we repeatedly found a moderate increase in the half-life of TCRα in Bag6 knockdown cells (Figure 4D). Thus, the accumulation of TCRα in Bag6 knockdown cells can be at least in part attributed to increased protein stability. In agreement with this notion, polyubiquitinated TCRα was accumulated in Bag6 knockdown cells (Figure 4E). Stabilization of TCRα was also seen when Ubl4A and Trc35 were individually knocked down (Figures 4F and 4G; Figure S4A),

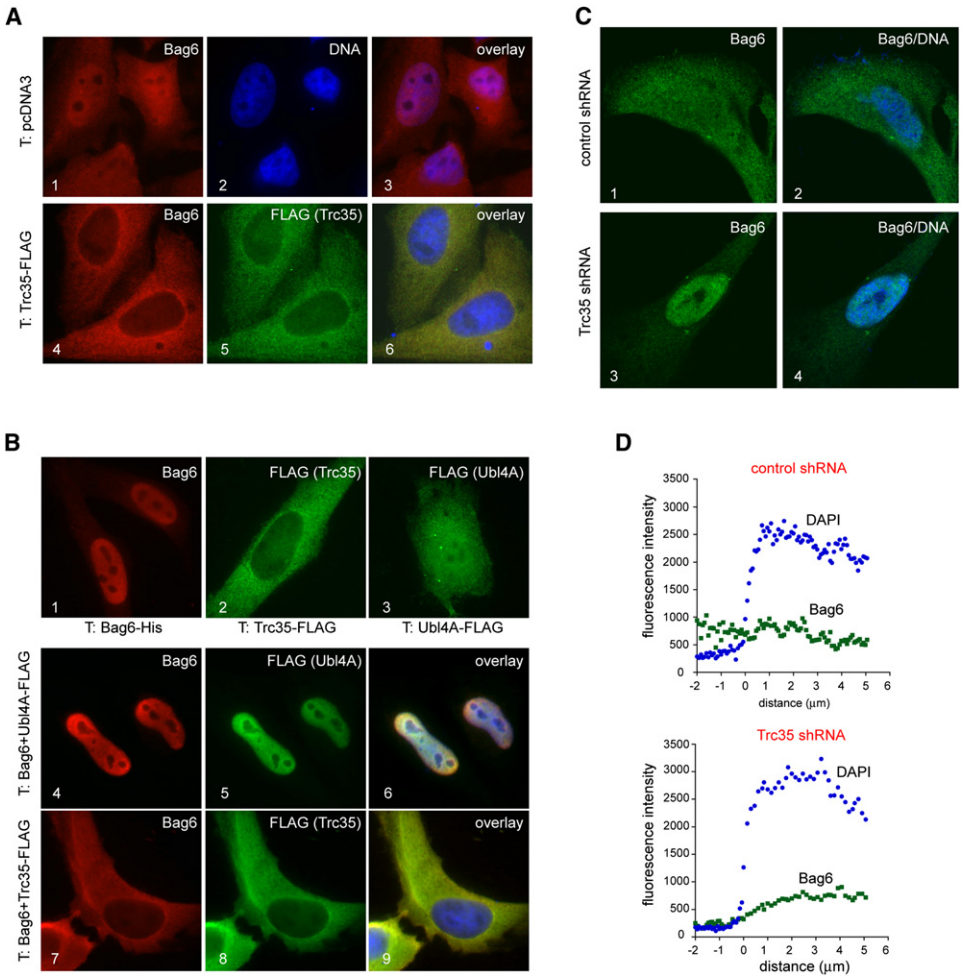

Figure 2. Trc35 Maintains a Cytosolic Pool of Bag6

(A) Trc35 expression alters the subcellular localization of endogenous Bag6. HeLa cells transfected (T) with a control vector (panels 1–3) or a Trc35-FLAG-expressing plasmid were stained with anti-Bag6 (red) and anti-FLAG (green) antibodies. Where indicated, DNA was stained with DAPI (blue).

(B) Trc35, but not Ubl4A, retains overexpressed Bag6 in the cytoplasm. HeLa cells transfected with the indicated plasmids either individually (panels 1–3) or in combination (panels 4–9) were stained to visualize Bag6 (red), FLAG-tagged proteins (green), and DNA (blue).

(C and D) Knockdown of Trc35 increases nuclear localization of Bag6. HeLa cells transfected with either a control or Trc35 shRNA construct were stained with a Bag6 antibody (red) and DAPI (blue). Shown are representative cells imaged by a confocal microscope. The graphs in (D) show the profiles of averaged Bag6 (green) and DAPI (blue) fluorescence intensity across the nuclear envelope boundary (indicated by position 0) measured by a confocal microscope (n = 10 cells). See also Figure S2.

suggesting that Bag6 acts in conjunction with these two cofactors to increase ERAD efficiency.

The ERAD defects associated with depletion of the Bag6 complex cannot be simply attributed to the previously proposed chaperoning function of Bag6 in biosynthesis of ER TA proteins such as the translocon component Sec61β or the ER-associated ubiquitin E2 enzyme Ube2j1 for the reasons outlined below. First, although the Bag6 complex can increase the efficiency and fidelity of membrane targeting for some TA proteins in vitro, an essential role in TA protein biogenesis in intact cells for Bag6 has not been demonstrated (Leznicki et al., 2010; Mariappan et al., 2010). In fact, yeast strains lacking either GET4 or GET5, the functional homologs of Trc35 and Ubl4A, respectively, are viable, whereas deletion of single ER TA proteins such as BOS1 can cause lethality. This strongly suggests that the Bag6 complex and its yeast functional ortholog are not absolutely essential for TA protein membrane targeting in the cell, as suggested previously (Mariappan et al., 2010). Consistent with this view, we found that TCRα accumulated in Bag6 knockdown cells comigrated with TCRα from control cells on a SDS-PAGE gel. This type I membrane protein apparently still carried N-glycan, which was confirmed by Endo H treatment (Figure 4H). Likewise, Endo H treatment also caused a shift in molecular weight of polyubiquitinated TCRα isolated from Bag6 knockdown cells (Figure S4B). Thus, TCRα accumulated in Bag6 knockdown cells must be originated from the ER. This scenario would not occur if knockdown of Bag6 had impaired membrane insertion of Sec61β. Second, neither the protein levels nor the solubility of

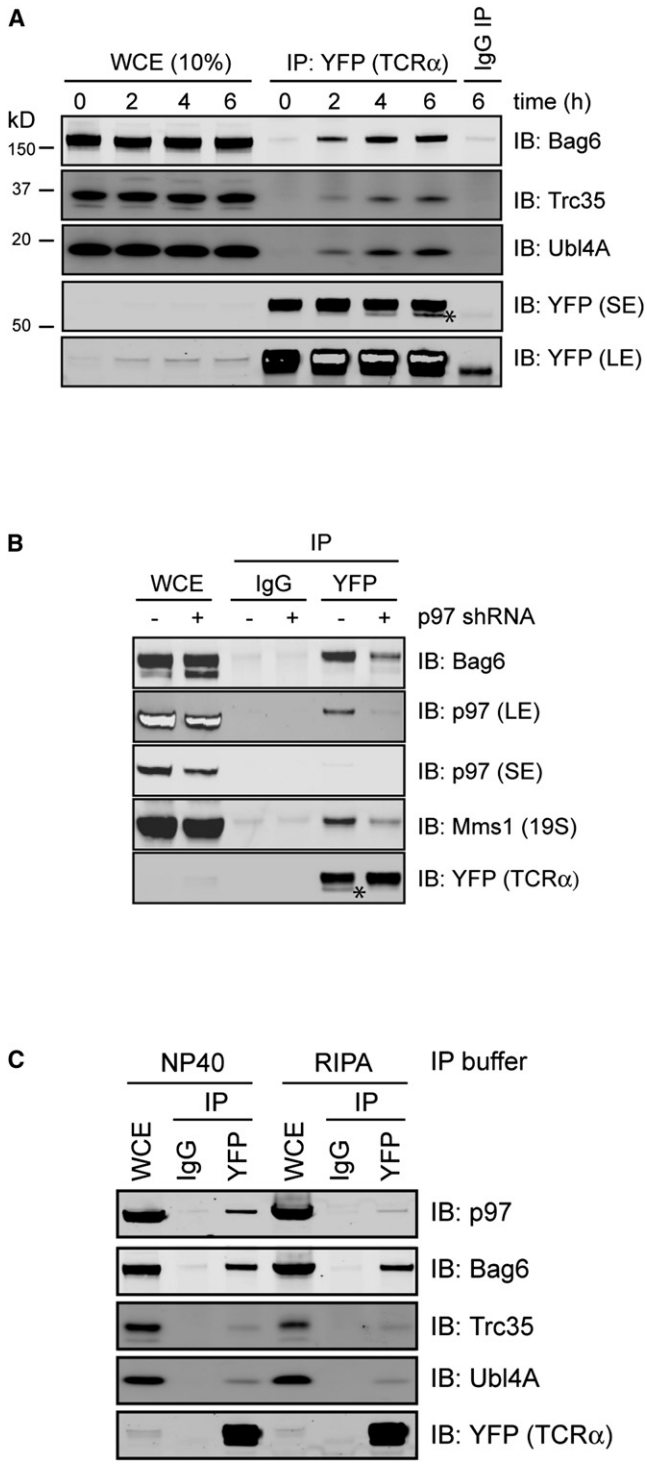

Figure 3. The Bag6 Complex Interacts with the Retrotranslocation Substrate TCRα

(A) 293T cells stably expressing YFP-tagged TCRα were treated with MG132 (20 μM) for the indicated time periods. TCRα-YFP-containing complexes were immunoprecipitated from NP40 lysis buffer-generated cell extracts and analyzed by immunoblotting. Where indicated, a fraction of the whole-cell extract (WCE) was analyzed directly by immunoblotting. Asterisk indicates a deglycosylated TCRα species. LE, long exposure; SE, short exposure.

(B) As in (A), except that siRNA-transfected cells were treated with MG132 for 6 hr.

(C) The Bag6-TCRα complex is stable in the RIPA buffer. 293T cells expressing YFP-tagged TCRα were treated with MG132 (20 μM) for 4 hr. Cells were lysed in either a NP40-containing lysis buffer or the RIPA buffer. Cell extracts were subject to immunoprecipitation and immunoblotting by the indicated antibodies. See also Figure S3.

Sec61β and Ube2j1 was affected by depletion of Bag6 or Ubl4A, even though ERAD defect under the same condition was manifest (Figures 4B and 4E; Figure S4A). These TA proteins are apparently targeted to the ER membranes in Bag6 knockdown cells, because otherwise they would be rapidly degraded by the proteasome due to the presence of the exposed TMD in the cytosol (Hessa et al., 2011). We therefore conclude that TA protein biogenesis is largely unaffected in cells containing reduced levels of the Bag6 complex. Perhaps a redundant mechanism(s) exists in the cell to ensure normal levels of TA protein biosynthesis in the absence of Bag6 (see below). Thus, the most plausible interpretation of our data is that the Bag6 complex has a direct function in ERAD independent of its role in TA protein biogenesis.

Bag6 Maintains the Solubility of ERAD Substrates

When Bag6 knockdown cells were examined by fluorescence microscopy, we noticed that the TCRα-YFP signal often displayed an uneven pattern with many bright speckles, indicative of protein aggregation (Figure S5A). Indeed, sequential extraction experiments showed that the NP40 insoluble pellet derived from Bag6 knockdown cells, but not from control cells, contained a large amount of TCRα, which could be resolubilized by the Laemmli buffer (Figure 5A). Pulse-chase experiment confirmed a time-dependent accumulation of TCRα in an NP40 insoluble form in Bag6 knockdown cells, which was not observed in control cells (Figure 5B, lanes 4–6 versus lanes 1–3). The TCRα aggregation phenotype was specifically associated with Bag6 depletion because knockdown of the dislocation driving ATPase p97 caused TCRα to accumulate primarily in NP40-soluble fractions (Figure 5C). In addition to TCRα, Bag6 depletion also caused other ERAD substrates, including CD4 (Magadan et al., 2010) and a TCRα variant lacking TMD (Soetandyo et al., 2010), to accumulate in NP40-insoluble fractions (Figure 5D; Figure S5B). By contrast, under the same Bag6 depletion condition, neither the ERAD machinery proteins such as gp78, p97, UbxD8, Derlin-2, and VIMP nor the ER resident proteins Sec61β and calnexin accumulated in NP40-insoluble fractions (Figure 5E). Together, these results suggest that Bag6 contains a chaperone-like activity that acts on ERAD substrates to maintain their solubility, which improves their degradation efficiency.

We next tested whether the Bag6-interacting proteins Trc35 and Ubl4A were required for the chaperone-like activity of Bag6 in the cell. Pulse-chase analyses demonstrated that TCRα-YFP also formed NP40-insoluble aggregates in Trc35 knockdown cells, and the kinetics of TCRα aggregation in Trc35 knockdown cells was comparable to that in Bag6-depleted cells (Figure 5B). This result was anticipated, given the established role of Trc35 in maintaining a cytosolic pool

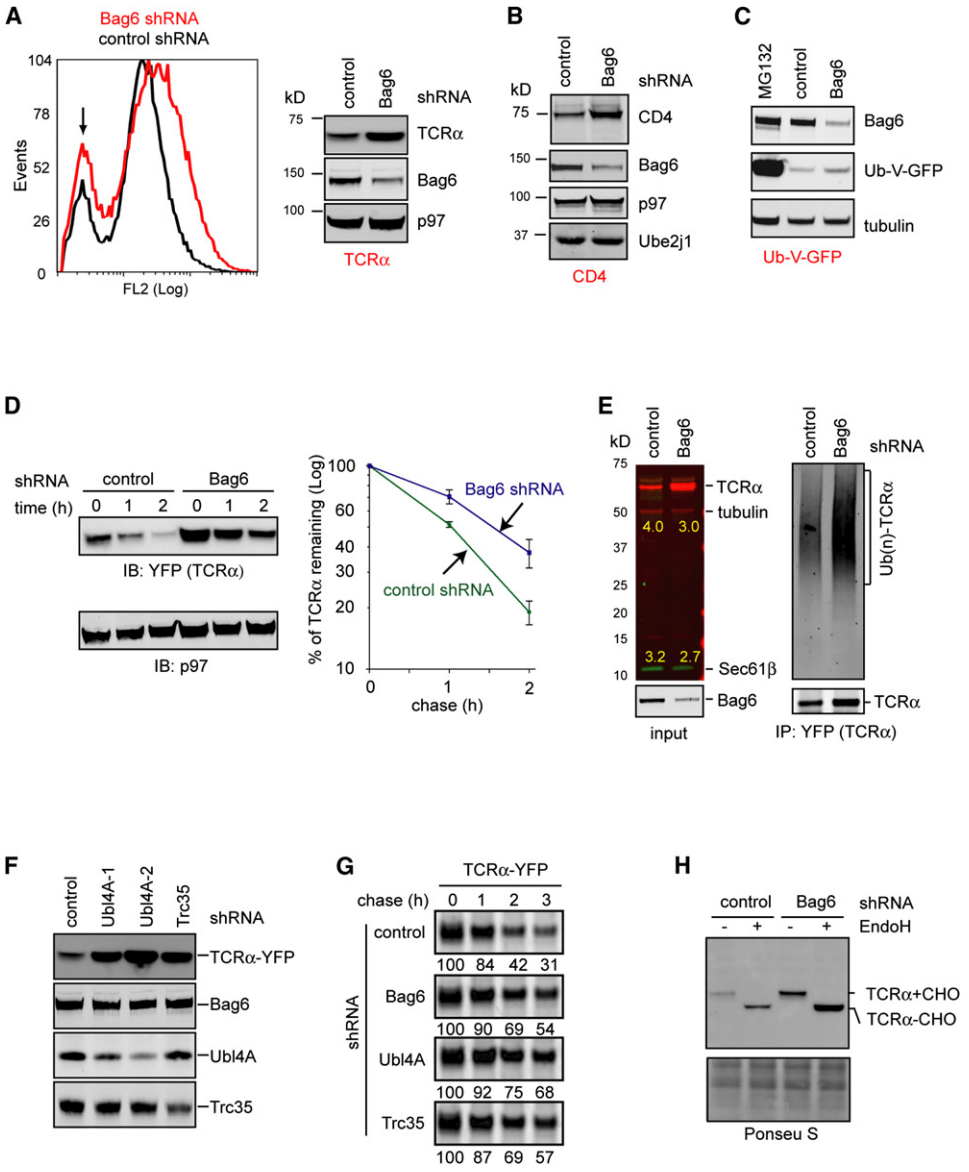

Figure 4. The Bag6 Complex Is Required for Efficient Degradation of Misfolded ER Proteins

(A) Knockdown of Bag6 stabilized TCRα. TCRα-YFP-expressing cells were transfected with the indicated shRNA constructs. TCRα-YFP levels in cells were determined by flow cytometry and immunoblotting. A small population of cells does not express TCRα-YFP, as indicated by the arrow. Unless specified, cell extracts were prepared using a NP40-containing lysis buffer.

(B) Cells expressing CD4 and Vpu were treated with the indicated shRNA. Whole-cell extracts were analyzed by immunoblotting with the indicated antibodies.

(C) As in (B), except that cells expressing Ub-V-GFP were used. Where indicated, cells were treated with MG132 (20 μM) for 12 hr.

(D) Cells expressing TCRα-YFP and the indicated shRNAs were subject to cycloheximide chase analyses to determine the half-life of TCRα. The graph shows the quantification results from three independent experiments. Error bars, SD (n = 3).

(E) TCRα accumulated in Bag6 knockdown cells in polyubiquitinated form. Where indicated, TCRα was immunoprecipitated under a denaturing condition and blotted for the indicated proteins.

(F) Knockdown of Ubl4A or Trc35 caused accumulation of TCRα in cells. Detergent extracts of TCRα-YFP-expressing cells transfected with the indicated shRNA constructs were analyzed by immunoblotting.

(G) Pulse-chase analysis of TCRα degradation in 293T cells expressing the indicated knockdown shRNAs together with TCRα. The numbers indicate the relative levels of TCRα.

(H) Whole-cell extracts prepared from TCRα-YFP-expressing cells transfected with the indicated shRNA constructs were treated with Endo H. See also Figure S4.

of Bag6 for engagement in ERAD (Figure 2). Intriguingly, knockdown of Ubl4A did not cause TCRα to accumulate in NP40-insoluble fractions (Figure 5B), despite the fact that its depletion had a strong inhibitory effect on ERAD (Figure 4G; Figure S4A). Thus, Ubl4A is dispensable for the chaperone function of Bag6, although its activity is strictly required for ERAD.

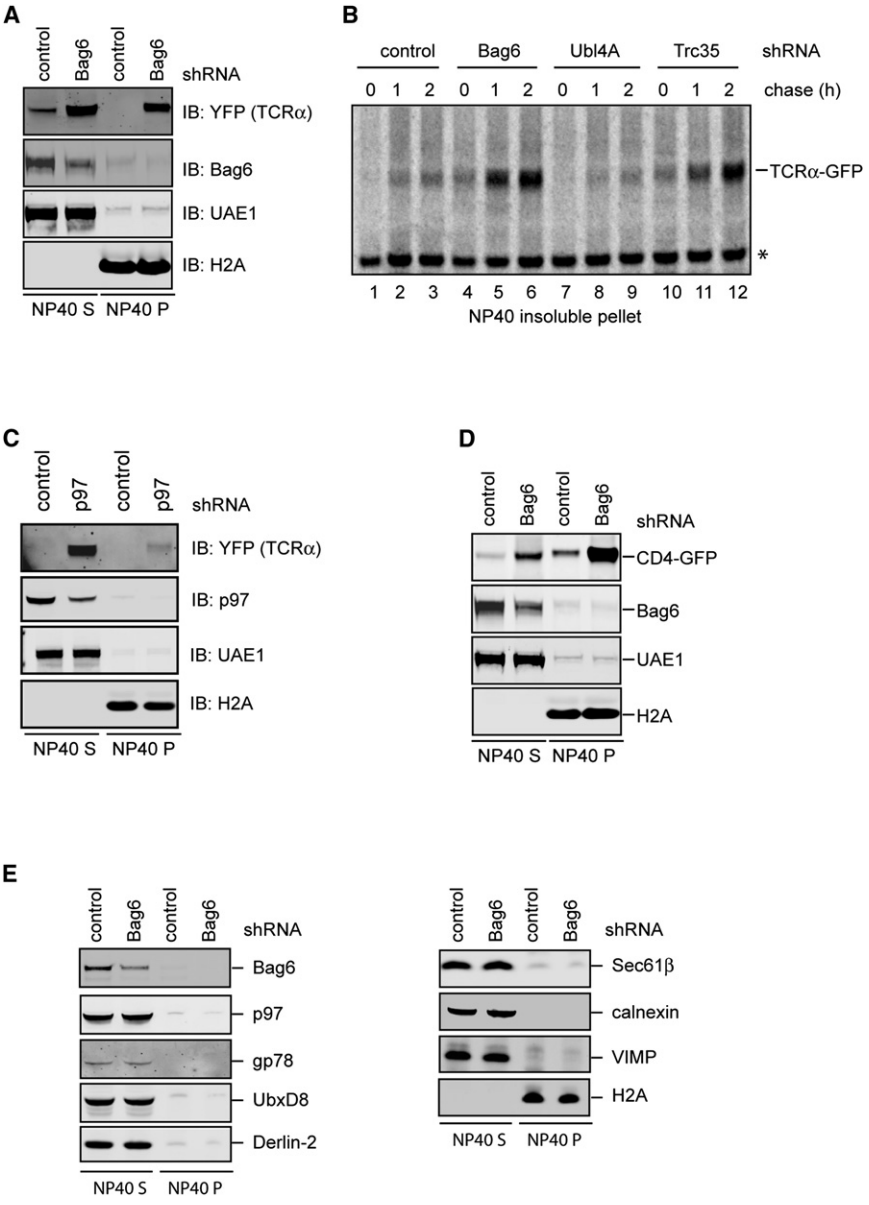

Figure 5. The Bag6 Complex Maintains the Solubility of ERAD Substrates to Facilitate Their Turnover

(A) TCRα accumulates in an NP40-insoluble state in Bag6 knockdown cells. Cells expressing TCRα-YFP and the indicated shRNAs were first extracted by the NP40 lysis buffer (NP40 S). The NP40-insoluble pellet fractions were resolubilized in the Laemmli buffer (NP40 P).

(B) Knockdown of the individual component of the Bag6 complex differentially affects the solubility of TCRα. 293T cells expressing TCRα-YFP and the indicated shRNAs were pulse labeled with ^{35}S-Met/Cys and then incubated in a medium containing excess unlabeled Met and Cys. The NP40 insoluble materials from the cells were resolubilized by a buffer containing 2% SDS and 5 mM DTT followed by dilution into the NP40 buffer before immunoprecipitation analyses.

(C) As in (A), except that cells transfected with a shRNA construct targeting p97 were analyzed.

(D) As in (A), except that cells expressing CD4-GFP and Vpu were used.

(E) As in (A), except that samples were immunoblotted with antibodies against the indicated proteins. See also Figure S5.

Bag6 Contains a Chaperone Holdase Activity

To understand the nature of the Bag6 chaperone activity, we tested whether purified recombinant Bag6 could prevent protein aggregation in vitro. We used luciferase as a model substrate because its thermodynamic instability caused it to aggregate at 42°C. To eliminate potential confounding effects from factors copurified with Bag6, particularly the previously reported Bag6-binding protein Hsp70 (Thress et al., 2001), we purified Bag6 from 293T cells to more than 90% homogeneity under a high-salt condition (Figure 6A). Immunoblotting showed no significant contamination of Hsp70 proteins in the purified Bag6 sample (Figure S6A). Light scattering experiments demonstrated a concentration-dependent suppression of luciferase aggregation by Bag6 (Figure 6B). This activity did not require the Bag6 UBL domain, because an UBL-deleted Bag6 mutant had a similar activity as wild-type Bag6. Moreover, ATP was not required, since the reactions did not contain any nucleotides. We also tested purified Ubl4A and found that it did not suppress luciferase aggregation. On the other hand, a purified Bag6-Ubl4A complex had a similar activity as Bag6 alone (Figure S6B). We were unable to test Trc35 in this assay because we could not purify Trc35 due to poor expression and solubility. Interestingly, when bovine serum albumin (BSA) was used as a negative control, it caused a small amount of luciferase to remain in soluble fractions after heating when compared to the buffer control (Figure S6C). The mechanism of this observation was unclear, but light scattering experiments showed that the effect BSA on luciferase aggregation was insignificant compared to that of Bag6 (Figure S6D).

Bag6 may suppress luciferase aggregation by promoting luciferase refolding or by sequestering it in an unfolded soluble state. To discriminate between these possibilities, we monitored the folding status of luciferase by measuring the luciferase activity after heat denaturation. If Bag6 promoted luciferase refolding, one would expect to detect more luciferase activity in the soluble fractions when Bag6 was present. As expected, incubation of luciferase at 42°C reduced its activity by 100-fold (Figure 6D, sample 6 versus input). The remaining luciferase activity likely resulted from spontaneous refolding after denaturation. Remarkably, despite the fact that more luciferase was present in the Bag6-containing supernatant fractions (Figure S6C; Figure 6C),

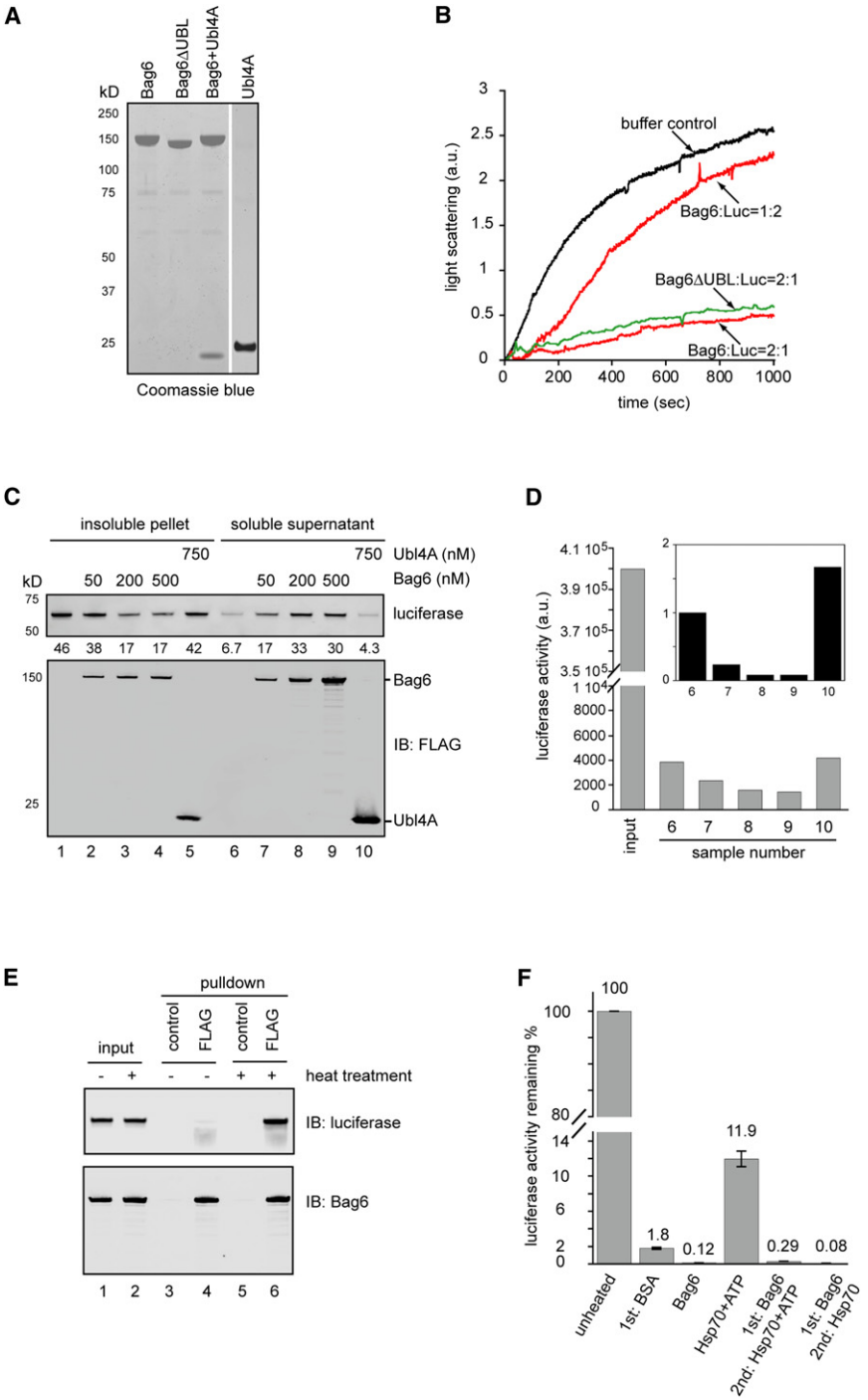

Figure 6. Bag6 Has a Chaperone Holdase Activity that Maintains an Aggregation-Prone Substrate in an Unfolded Soluble State

(A) A Coomassie blue-stained gel shows the purified proteins.

(B) Bag6 suppresses luciferase aggregation. Luciferase (150 nM) was incubated with either buffer or the indicated amount of purified Bag6 or a UBL domain-deleted Bag6 mutant (ΔUBL) at 42°C. The scattered light at 330 nm was measured by a spectrometer.

(C) Luciferase (150 nM) was incubated with either buffer or the indicated amount of purified proteins at 42°C for 20 min. Luciferase aggregates were sedimented by centrifugation. The pellet and supernatant fractions were analyzed by immunoblotting. The numbers show the relative luciferase level.

(D) The luciferase activity in the supernatant fractions from (C) was determined. Input shows the activity of an equal amount of native luciferase. The inset shows the relative luciferase activity normalized by protein levels determined in (C).

(E) Bag6 binds denatured luciferase. Luciferase was incubated with Bag6 at a 1:2 molar ratio either on ice (–) or at 42°C (+) for 20 min. Soluble fractions were subject to immunoprecipitation with FLAG antibody to pull down Bag6.

(F) Luciferase captured by Bag6 cannot be refolded by Hsp70. Luciferase (80 nM) was heat inactivated in the presence of BSA (160 nM), Bag6 (160 nM), or a Hsp70 chaperone mixture containing Hsp70 (150 nM), HOP (200 nM), Hdj1 (300 nM), and ATP 5 mM. After denaturation, samples were incubated at 25°C for 30 min. Where indicated, the same Hsp70 chaperone mixture was added with or without ATP during the second incubation. Error bars indicate the mean of two independent experiments. See also Figure S6.

lesser activity was detected (Figure 6D, samples 7–9 versus samples 6 and 10). We thus conclude that denatured luciferase in Bag6-containing samples remains unfolded and must be still bound by Bag6. Indeed, an interaction between heat-denatured luciferase and Bag6 could be readily detected by coimmunoprecipitation, whereas native luciferase failed to bind Bag6 (Figure 6E). Because incubation of the luciferase-Bag6 complex with an Hsp70 folding system comprising purified Hdj1, HOP, and Hsp70 did not lead to significant luciferase refolding (Figure 6F), luciferase captured by Bag6 apparently could not be spontaneously released. Intriguingly, when Bag6 and Hsp70 were present at the same time during luciferase denaturation, substoichiometric amount of Bag6 (the ratio of Bag6:Hsp70 at 1:8) could inhibit the refolding activity of Hsp70 by ~80% (Figure S6E). This is most likely due to competition of Bag6 and Hsp70 for substrate binding. Taken together, our results suggest that Bag6 does not act as a conventional chaperone that assists proteins in folding. Instead, it functions as a molecular holdase that binds denatured polypeptides to sequester them in an unfolded yet soluble state.

Bag6 Is Involved in US11-Induced ERAD

To further demonstrate that the Bag6 complex is directly involved in ERAD, we tested whether the Bag6 complex was

required for the degradation of MHC class I HC in permeabilized A9 cells. A9 cells stably expressed the HCMV protein US11 and a hemagglutinin (HA)-tagged HC (HLA-A2). Under the influence of US11, newly synthesized HC is constantly degraded by the ERAD pathway (Shamu et al., 1999). We and others have previously established an in vitro permeabilized cell assay that recapitulates HC degradation in vivo (Shamu et al., 1999; Soetandyo and Ye, 2010; Ye et al., 2001). The assay used a low concentration of the detergent digitonin to permeabilize the plasma membrane of the cells that contain radiolabeled nascent HC. This allows efficient removal of the cytosol by centrifugation. The degradation of HC can be reconstituted by incubating the membrane fraction with cytosol of a defined source in the presence of ATP and ubiquitin (Figure S7A). To test the involvement of the Bag6 complex in this process, we treated permeabilized A9 cells with high salt, which removed most membrane-bound Bag6 complex (data not shown). We then incubated the membrane with either mock depleted cow liver cytosol (CLC) or CLC depleted of the Bag6 complex using an Ubl4A antibody (Figure 7A). HC was rapidly degraded when A9 cell-derived membranes were incubated with control CLC. In contrast, HC degradation was significantly attenuated when Bag6-depleted CLC was used (Figures 7B and 7C).

Because we could not purify Trc35 and perform an add-back experiment to rectify the ERAD defect associated with depletion of the Bag6 complex, we further examined the role of Bag6 in US11-induced ERAD by analyzing its interaction with HC. Similar to TCRα, a significant fraction of Bag6 could be coprecipitated with HC in proteasome-inhibited cells (Figure 7D). Importantly, proteasome inhibition caused the accumulation of a deglycosylated HC species (Figure 7D) that comprised a membrane-bound retrotranslocation intermediate and a fully dislocated species in the cytosol (Figure 7E). Fractionation experiments showed that Bag6 interacted with HC both in the membrane and in the cytosol (Figure 7E). Because only deglycosylated HC specifically coprecipitated with Bag6 (Figure 7F, Figure S7B), Bag6 must bind a HC dislocation intermediate at the ER membrane and accompany it into the cytosol for proteasome degradation. Quantification of the binding experiment showed that ~25% of the dislocated HC was captured by Bag6 (Figure 7F). This was unlikely to be caused by dissociation of HC from Bag6 during immunoprecipitation, given the strong interaction of Bag6 with substrates (Figure 3C; Figure 6F). Thus, another cytosolic holdase(s) may act in parallel with Bag6 to capture dislocated HC. Collectively, the ERAD defect associated with Bag6 depletion and the physical interaction of retrotranslocated HC with Bag6 strongly suggest that Bag6 is directly involved in US11-induced retrotranslocation.

DISCUSSION

A Chaperoning Role for Bag6 in ERAD

In this study, we establish the Bag6-Ubl4A-Trc35 complex as a key mediator in a previously unknown chaperoning step in ERAD. We show that the ERAD substrate TCRα accumulates in polyubiquitinated form in Bag6-depleted cells. Moreover, since the association of Bag6 with TCRα is reduced upon p97 depletion, Bag6 likely acts downstream of p97-mediated dislocation. Our characterization of Bag6 interaction with the retrotranslocation substrate HC further supports this conclusion. As a type I membrane protein carrying a single N-glycan in its ER luminal domain, HC is retrotranslocated in glycosylated form. Once emerged from a putative retrotranslocon, deglycosylation occurs rapidly by a cytosolic N-glycanase. The deglycosylated HC is then released into the cytosol for degradation by the proteasome (Blom et al., 2004; Shamu et al., 1999). Unlike many other ERAD substrates, retrotranslocation and degradation of HC can be uncoupled (Wiertz et al., 1996). When the proteasome function is impaired, HC accumulates in the cytosol as a fully dislocated degradation intermediate lacking N-glycan. We show that Bag6 preferentially interacts with deglycosylated HC both on the membrane and in the cytosol. Therefore, the initial substrate binding by Bag6 likely occurs on the membrane while HC is undergoing retrotranslocation and deglycosylation. Bag6 may even be required for deglycosylation because both TCRα and HC are stabilized entirely in the sugar-containing form when Bag6 was knocked down. Since the translocation-driving ATPase p97 does not form stable interactions with the proteasome, ERAD substrates are thought to be transferred from p97 to the proteasome via some shuttling factors (Hirsch et al., 2009; Vembar and Brodsky, 2008). Our data suggest that Bag6 may be an integral part of a shuttling system, which recognizes a retrotranslocation intermediate on the ER membrane and accompanies it to the proteasome (Figure 7G). In this regard, it is conceivable that ERAD substrates with slow transport kinetics or those carrying strong hydrophobic motifs may be particularly prone to aggregation in the cytosol, and therefore be more dependent on a holdase to maintain solubility while being targeted to the proteasome.

Efficient degradation of misfolded ER proteins also requires the two Bag6 cofactors, Trc35 and Ubl4A. Our results suggest that one function of Trc35 is to maintain a cytosolic pool of Bag6 that can participate in ERAD, but our data do not exclude the possibility that Trc35 may have other functions essential for the holdase activity of Bag6 in the cell. The function of Ubl4A in ERAD is unclear. In budding yeast, GET5 and GET4 appear to regulate substrate handoff from Sgt2, a functional counterpart of Bag6, to the downstream chaperone GET3 (Jonikas et al., 2009; Wang et al., 2010). Ubl4A may have a similar role in substrate handoff to the proteasome, which would explain the lack of protein aggregation in Ubl4A knockdown cells.

Bag6 Is a Multifunctional Chaperone Holdase

We demonstrate that Bag6, the central component of the Bag6 complex, can maintain the solubility of ERAD substrates to improve degradation efficiency. This function is consistent with the holdase activity of Bag6, which is demonstrated using an in vitro assay. The holdase activity allows Bag6 to maintain substrates in an unfolded yet soluble state, which makes them preferred substrates of the proteasome because the proteasome cannot efficiently digest protein aggregates (Venkatraman et al., 2004).

Our finding that Bag6 acts as a holdase unifies the various facets of Bag6 functions around a common theme, and explains how Bag6 can operate in an array of seemingly unrelated biological processes. In essence, the holdase activity of Bag6 can

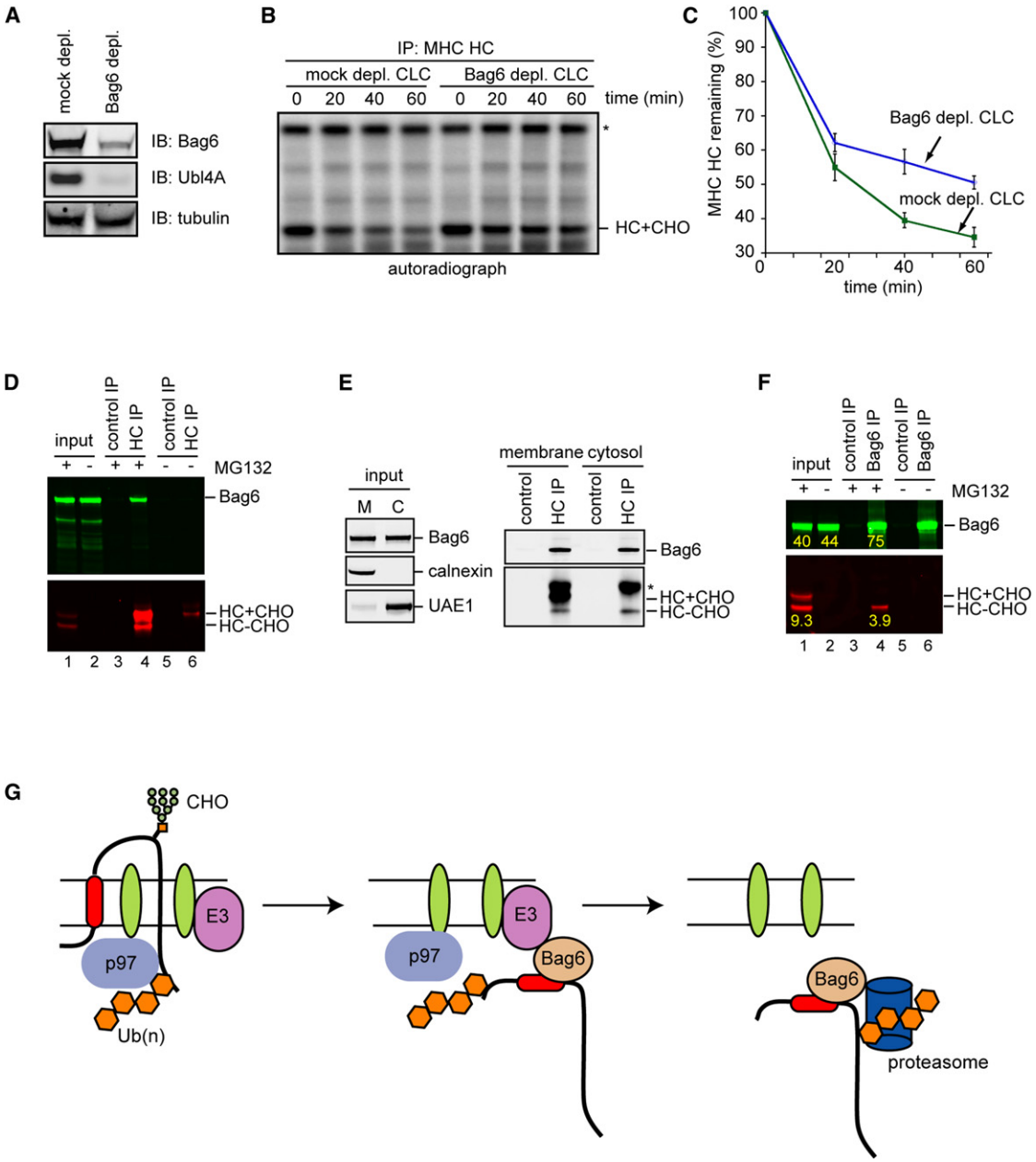

Figure 7. Bag6 Is Involved in US11-Induced ERAD of MHC Class I HC

(A) Depletion of the Bag6 complex from CLC was confirmed by immunoblotting with antibodies against Bag6 and Ubl4A.

(B) Depletion of the Bag6 complex attenuates the degradation of HC in permeabilized A9 cells. Experiments were performed as outlined in Figure S7A. Asterisk indicates a nonspecific band.

(C) Quantification of HC turnover from three independent experiments. Error bars, SD (n = 3).

(D) Bag6 interacts with HC in US11 cells. HC+CHO and HC-CHO indicate glycosylated and deglycosylated HC, respectively.

(E) Bag6 binds HC both at the ER membrane and in the cytosol. MG132-treated A9 cells were permeabilized by the detergent digitonin. Cells were then fractionated into a membrane (M) and a cytosol (C) fraction before immunoprecipitation and immunoblotting analysis. Asterisk indicates IgG.

(F) Bag6 specifically interacts with deglycosylated HC. As in (D), except that immunoprecipitation was performed with anti-Bag6 antibody. The number shows the fluorescence intensity of the indicated bands.

(G) A model for the role of the Bag6 complex in ERAD. Association of Bag6 with ER-bound E3s positions it in proximity to substrates undergoing retrotranslocation, which allows Bag6 to efficiently capture dislocated substrates bearing aggregation-prone hydrophobic motifs or TMD. Bag6 may escort substrates to the proteasome to enhance degradation efficiency. See also Figure S7.

shield hydrophobic patches or TMDs on diverse substrates, allowing them to be safely delivered to different cellular destinations without forming aggregation. In ERAD, the association of Bag6 with an ER-bound E3 renders it a preferred chaperone for capturing retrotranslocated polypeptides containing exposed aggregation-prone motifs. The substrates might remain bound to Bag6 until the chaperone-substrate complex encounters the proteasome or its associated ubiquitin receptors. This activity can be similarly employed to degrade misfolded cytosolic proteins (Minami et al., 2010) or cytosol-derived mislocalized membrane proteins including defective TA proteins carrying hydrophobic TMD (Hessa et al., 2011). The holdase concept also explains the proposed role of Bag6 and of its yeast counterpart Sgt2 in TA protein biogenesis (Mariappan et al., 2010; Wang et al., 2010). In this process, Bag6 holds ribosome-released nascent chains bearing aggregation-prone tail anchor to facilitate their membrane insertion.

Substrate Recognition by Bag6

Bag6 was recently shown to interact with polyubiquitinated proteins in the cell (Minami et al., 2010). However, Bag6 does not contain any ubiquitin-binding activity by itself (Figure S6F). Thus, the interaction of Bag6 with retrotranslocation substrates must be mediated by a nonmodified segment in substrates.

During TA protein biogenesis, Bag6 acts as a TMD-selective chaperone that preferentially binds exposed TMD in substrates (Mariappan et al., 2010). Our results show that in the context of ERAD, TMD is not a prerequisite for Bag6 engagement because the degradation of a TMD-deleted TCRα variant also involves Bag6. We propose that substrate recognition by Bag6 may involve a long stretch of hydrophobic residues, but not necessarily a TMD. This type of motif is present in many dislocated soluble ERAD substrates that are unfolded during retrotranslocation. For example, the TMD-deleted TCRα contains several long stretches of hydrophobic residues, which may be the binding site(s) for Bag6. Our model is supported by several lines of evidence. First, the soluble protein luciferase, once unfolded, can be directly recognized by Bag6. Additionally, the degradation of a model proteasome substrate carrying a hydrophobic degron (not a TMD) fused to GFP is dependent on Bag6 (Minami et al., 2010), whereas the degradation of a folded substrate Ub-V-GFP does not require Bag6, presumably because it does not contains any exposed hydrophobic motifs. Lastly, Bag6 is known to have functions in the nucleus where no membrane protein is present (Nguyen et al., 2008).

If Bag6 recognizes hydrophobic segments in substrates, it needs to compete with a large number of cytosolic chaperones, which bind substrates via a similar manner (Bukau et al., 2006). Several mechanisms may act together to ensure efficient capture of substrates by Bag6. First, the difference in hydrophobicity may offer a gauge for chaperones to distinguish between different substrates. For example, Hsp70 is known to recognize substrates carrying short hydrophobic segments. A long hydrophobic segment in a substrate may increase its affinity to Bag6, making it a preferred chaperone. In agreement with this idea, luciferase contains at least two long stretches of hydrophobic residues, which explains why Bag6 can effectively compete with Hsp70 to capture denatured luciferase even at a concentration substantially lower than Hsp70. Second, the association of Bag6 with distinct cellular partners may further govern substrate recognition. It is possible that the interaction of Bag6 with the ribosome allows Bag6 to efficiently recognize nascent TA proteins (Mariappan et al., 2010), whereas its association with ER-anchored E3s could give Bag6 an edge over other competing chaperones even for binding to soluble substrates carrying a lesser hydrophobic motif.

The Redundancy of the Holdase Systems

Our results suggest that different ERAD substrates may have different levels of dependence on Bag6 function for degradation. For example, knockdown of Bag6 significantly stabilizes TCRα, but depletion of the Bag6 only moderately attenuates HC degradation in US11 cells. It is possible that another chaperone holdase may substitute Bag6 function to support HC degradation. Consistent with this interpretation, we found that only a fraction of the dislocated HC is bound to Bag6, although the presence of a TMD in this substrate predicts that all dislocated HC molecules should be accompanied by a holdase in the cytosol. Our results also show that knockdown of Bag6 does not have an apparent effect on the biogenesis of ER TA proteins, which further suggests the existence of multiple holdase systems with overlapping substrate specificity in the cell. This would also explain why yeast deletion mutants lacking GET4 and GET5 are viable, whereas deletion of many TA proteins singularly can often result in lethality.

EXPERIMENTAL PROCEDURES

Gene Knockdown and Various ERAD Assays

To knock down Bag6 and its associated cofactors, 293T cells were transfected with a gene-specific shRNA construct using Lipofectamine 2000 on day 1 and day 2. Seventy-two hours after the first transfection, cells were harvested for various assays. For pulse-chase experiments, 3.0×10^6 cells were harvested and incubated in 8 ml starvation DMEM medium free of Met/Cys for 60 min, and then incubated in 0.3 ml starvation medium containing 75 μCi ^{35}S-Met/Cys for 30 min. Cells were then incubated in a chase medium containing unlabeled Met (2.5 mM) and Cys (1 mM). 0.5×10^6 cells were removed at the indicated time points. Cell extracts were prepared in the NP40 lysis buffer. TCRα-YFP was immunoprecipitated using a GFP antibody. For cycloheximide chase experiments, cells treated with a DMEM medium containing 50 μg/ml cycloheximide were harvested at different time points. Cell extracts were prepared in the NP40 lysis buffer for analyses by immunoblotting. To analyze the in vivo aggregation of ERAD substrates, cells transfected with plasmids that expressed various ERAD substrates together with shRNA knockdown constructs were first solubilized in the NP40 lysis buffer. The detergent-insoluble fractions were further solubilized by the Laemmli buffer. To perform in vitro retrotranslocation assay, radiolabeled A9 cells were treated with a low concentration of the detergent digitonin to remove cytosol. Membranes were then washed and incubated with either mock-depleted or Bag6-depleted cytosol to initiate HC retrotranslocation.

Miscellaneous Biochemical Assays

Luciferase (150 nM) was incubated with Bag6 or other proteins at concentrations specified in the figure legends in a buffer containing 20 mM HEPES 7.4, 5 mM MgOAC, 50 mM KCl, 1 mM DTT. The samples were heated at 42°C, and the scattered light was measured at 330 nm using an AB2 luminescence spectrometer (Thermo Scientific). Alternatively, the samples were subject to centrifugation at 20,000 g for 10 min. The pellet and supernatant fractions were analyzed by immunoblotting. Luciferase activity was measured using a luciferase reporter gene assay kit from Roche. Depletion of the Bag6 complex

was performed as follows. Protein A agarose was first incubated with 1 ml anti-Ubl4A serum or control IgG and then with 1 ml CLC (~40 mg/ml). This procedure was repeated one more time to deplete more than 90% of the Bag6 complex. Endo H digestion experiments were carried out by incubating cell extracts containing 0.5% SDS with 2 μl Endo H (New England BioLab) in the presence of 1× reaction buffer (50 mM sodium citrate [pH 5.5]) at 37°C for 2 hr.

Additional methods are available in the Supplemental Information.

SUPPLEMENTAL INFORMATION

Supplemental Information includes seven figures, Supplemental Experimental Procedures, and Supplemental References and can be found with this article online at doi:10.1016/j.molcel.2011.05.010.

ACKNOWLEDGMENTS

We thank S. Fang (University of Maryland, Baltimore, MD) for reagents, and Michael Krause and Martin Gellert (National Institute of Diabetes and Digestive and Kidney Diseases [NIDDK]) and Tom Rapoport (Harvard Medical School) for critical reading of the manuscript. The research is supported by the National Institutes of Health Intramural AIDS Targeted Antiviral Program (IATAP) and by the Intramural Research Program of the NIDDK.

Received: December 29, 2010
Revised: March 14, 2011
Accepted: May 18, 2011
Published online: June 2, 2011

REFERENCES

Alexandru, G., Graumann, J., Smith, G.T., Kolawa, N.J., Fang, R., and Deshaies, R.J. (2008). UBXD7 binds multiple ubiquitin ligases and implicates p97 in HIF1alpha turnover. Cell *134*, 804–816.

Bays, N.W., Wilhovsky, S.K., Goradia, A., Hodgkiss-Harlow, K., and Hampton, R.Y. (2001). HRD4/NPL4 is required for the proteasomal processing of ubiquitinated ER proteins. Mol. Biol. Cell *12*, 4114–4128.

Bernardi, K.M., Forster, M.L., Lencer, W.I., and Tsai, B. (2008). Derlin-1 facilitates the retro-translocation of cholera toxin. Mol. Biol. Cell *19*, 877–884.

Bhamidipati, A., Denic, V., Quan, E.M., and Weissman, J.S. (2005). Exploration of the topological requirements of ERAD identifies Yos9p as a lectin sensor of misfolded glycoproteins in the ER lumen. Mol. Cell *19*, 741–751.

Blom, D., Hirsch, C., Stern, P., Tortorella, D., and Ploegh, H.L. (2004). A glycosylated type I membrane protein becomes cytosolic when peptide: N-glycanase is compromised. EMBO J. *23*, 650–658.

Buchberger, A., Bukau, B., and Sommer, T. (2011). Protein quality control in the cytosol and the endoplasmic reticulum: brothers in arms. Mol. Cell *40*, 238–252.

Bukau, B., Weissman, J., and Horwich, A. (2006). Molecular chaperones and protein quality control. Cell *125*, 443–451.

Chen, B., Mariano, J., Tsai, Y.C., Chan, A.H., Cohen, M., and Weissman, A.M. (2006). The activity of a human endoplasmic reticulum-associated degradation E3, gp78, requires its Cue domain, RING finger, and an E2-binding site. Proc. Natl. Acad. Sci. USA *103*, 341–346.

Desmots, F., Russell, H.R., Lee, Y., Boyd, K., and McKinnon, P.J. (2005). The reaper-binding protein scythe modulates apoptosis and proliferation during mammalian development. Mol. Cell. Biol. *25*, 10329–10337.

Fang, S., Ferrone, M., Yang, C., Jensen, J.P., Tiwari, S., and Weissman, A.M. (2001). The tumor autocrine motility factor receptor, gp78, is a ubiquitin protein ligase implicated in degradation from the endoplasmic reticulum. Proc. Natl. Acad. Sci. USA *98*, 14422–14427.

Hessa, T., Sharma, A., Mariappan, M., Eshleman, H.D., Gutierrez, E., and Hegde, R.S. (2011). Protein targeting and degradation pathways are coupled for elimination of misfolded proteins. Nature, in press.

Hirsch, C., Gauss, R., Horn, S.C., Neuber, O., and Sommer, T. (2009). The ubiquitylation machinery of the endoplasmic reticulum. Nature *458*, 453–460.

Jarosch, E., Taxis, C., Volkwein, C., Bordallo, J., Finley, D., Wolf, D.H., and Sommer, T. (2002). Protein dislocation from the ER requires polyubiquitination and the AAA-ATPase Cdc48. Nat. Cell Biol. *4*, 134–139.

Jonikas, M.C., Collins, S.R., Denic, V., Oh, E., Quan, E.M., Schmid, V., Weibezahn, J., Schwappach, B., Walter, P., Weissman, J.S., and Schuldiner, M. (2009). Comprehensive characterization of genes required for protein folding in the endoplasmic reticulum. Science *323*, 1693–1697.

Lee, S.O., Cho, K., Cho, S., Kim, I., Oh, C., and Ahn, K. (2010). Protein disulphide isomerase is required for signal peptide peptidase-mediated protein degradation. EMBO J. *29*, 363–375.

Leznicki, P., Clancy, A., Schwappach, B., and High, S. (2010). Bat3 promotes the membrane integration of tail-anchored proteins. J. Cell Sci. *123*, 2170–2178.

Li, W., Tu, D., Brunger, A.T., and Ye, Y. (2007). A ubiquitin ligase transfers preformed polyubiquitin chains from a conjugating enzyme to a substrate. Nature *446*, 333–337.

Lilley, B.N., and Ploegh, H.L. (2004). A membrane protein required for dislocation of misfolded proteins from the ER. Nature *429*, 834–840.

Lilley, B.N., and Ploegh, H.L. (2005). Viral modulation of antigen presentation: manipulation of cellular targets in the ER and beyond. Immunol. Rev. *207*, 126–144.

Magadan, J.G., Perez-Victoria, F.J., Sougrat, R., Ye, Y., Strebel, K., and Bonifacino, J.S. (2010). Multilayered mechanism of CD4 downregulation by HIV-1 Vpu involving distinct ER retention and ERAD targeting steps. PLoS Pathog. *6*, e1000869. 10.1371/journal.ppat.1000869.

Mariappan, M., Li, X., Stefanovic, S., Sharma, A., Mateja, A., Keenan, R.J., and Hegde, R.S. (2010). A ribosome-associating factor chaperones tail-anchored membrane proteins. Nature *466*, 1120–1124.

Minami, R., Hayakawa, A., Kagawa, H., Yanagi, Y., Yokosawa, H., and Kawahara, H. (2010). BAG-6 is essential for selective elimination of defective proteasomal substrates. J. Cell Biol. *190*, 637–650.

Nguyen, P., Bar-Sela, G., Sun, L., Bisht, K.S., Cui, H., Kohn, E., Feinberg, A.P., and Gius, D. (2008). BAT3 and SET1A form a complex with CTCFL/BORIS to modulate H3K4 histone dimethylation and gene expression. Mol. Cell. Biol. *28*, 6720–6729.

Nishikawa, S.I., Fewell, S.W., Kato, Y., Brodsky, J.L., and Endo, T. (2001). Molecular chaperones in the yeast endoplasmic reticulum maintain the solubility of proteins for retrotranslocation and degradation. J. Cell Biol. *153*, 1061–1070.

Okuda-Shimizu, Y., and Hendershot, L.M. (2007). Characterization of an ERAD pathway for nonglycosylated BiP substrates, which require Herp. Mol. Cell *28*, 544–554.

Rabinovich, E., Kerem, A., Frohlich, K.U., Diamant, N., and Bar-Nun, S. (2002). AAA-ATPase p97/Cdc48p, a cytosolic chaperone required for endoplasmic reticulum-associated protein degradation. Mol. Cell. Biol. *22*, 626–634.

Ron, D., and Walter, P. (2007). Signal integration in the endoplasmic reticulum unfolded protein response. Nat. Rev. Mol. Cell Biol. *8*, 519–529.

Schulze, A., Standera, S., Buerger, E., Kikkert, M., van Voorden, S., Wiertz, E., Koning, F., Kloetzel, P.M., and Seeger, M. (2005). The ubiquitin-domain protein HERP forms a complex with components of the endoplasmic reticulum associated degradation pathway. J. Mol. Biol. *354*, 1021–1027.

Shamu, C.E., Story, C.M., Rapoport, T.A., and Ploegh, H.L. (1999). The pathway of US11-dependent degradation of MHC class I heavy chains involves a ubiquitin-conjugated intermediate. J. Cell Biol. *147*, 45–58.

Shen, Y., Ballar, P., and Fang, S. (2006). Ubiquitin ligase gp78 increases solubility and facilitates degradation of the Z variant of alpha-1-antitrypsin. Biochem. Biophys. Res. Commun. *349*, 1285–1293.

Soetandyo, N., and Ye, Y. (2010). The p97 ATPase dislocates MHC class I heavy chain in US2 expressing cells via an Ufd1-Npl4 independent mechanism. J. Biol. Chem. *285*, 32352–32359.

Soetandyo, N., Wang, Q., Ye, Y., and Li, L. (2010). Role of intramembrane charged residues in the quality control of unassembled T-cell receptor alpha-chains at the endoplasmic reticulum. J. Cell Sci. *123*, 1031–1038.

Song, B.L., Sever, N., and DeBose-Boyd, R.A. (2005). Gp78, a membrane-anchored ubiquitin ligase, associates with Insig-1 and couples sterol-regulated ubiquitination to degradation of HMG CoA reductase. Mol. Cell *19*, 829–840.

Thress, K., Song, J., Morimoto, R.I., and Kornbluth, S. (2001). Reversible inhibition of Hsp70 chaperone function by Scythe and Reaper. EMBO J. *20*, 1033–1041.

Ushioda, R., Hoseki, J., Araki, K., Jansen, G., Thomas, D.Y., and Nagata, K. (2008). ERdj5 is required as a disulfide reductase for degradation of misfolded proteins in the ER. Science *321*, 569–572.

Vembar, S.S., and Brodsky, J.L. (2008). One step at a time: endoplasmic reticulum-associated degradation. Nat. Rev. Mol. Cell Biol. *9*, 944–957.

Venkatraman, P., Wetzel, R., Tanaka, M., Nukina, N., and Goldberg, A.L. (2004). Eukaryotic proteasomes cannot digest polyglutamine sequences and release them during degradation of polyglutamine-containing proteins. Mol. Cell *14*, 95–104.

Wang, F., Brown, E.C., Mak, G., Zhuang, J., and Denic, V. (2010). A chaperone cascade sorts proteins for posttranslational membrane insertion into the endoplasmic reticulum. Mol. Cell *40*, 159–171.

Wiertz, E.J., Jones, T.R., Sun, L., Bogyo, M., Geuze, H.J., and Ploegh, H.L. (1996). The human cytomegalovirus US11 gene product dislocates MHC class I heavy chains from the endoplasmic reticulum to the cytosol. Cell *84*, 769–779.

Ye, Y., Meyer, H.H., and Rapoport, T.A. (2001). The AAA ATPase Cdc48/p97 and its partners transport proteins from the ER into the cytosol. Nature *414*, 652–656.

Ye, Y., Shibata, Y., Yun, C., Ron, D., and Rapoport, T.A. (2004). A membrane protein complex mediates retro-translocation from the ER lumen into the cytosol. Nature *429*, 841–847.

Zhong, X., Shen, Y., Ballar, P., Apostolou, A., Agami, R., and Fang, S. (2004). AAA ATPase p97/valosin-containing protein interacts with gp78, a ubiquitin ligase for endoplasmic reticulum-associated degradation. J. Biol. Chem. *279*, 45676–45684.

Molecular Cell, Volume *42*

Supplemental Information

A Ubiquitin Ligase-Associated Chaperone Holdase Maintains Polypeptides in Soluble States for Proteasome Degradation

Qiuyan Wang, Yanfen Liu, Nia Soetandyo, Kheewoong Baek, Ramanujan Hegde, and Yihong Ye

Inventory of Supplemental Information

Supplemental Figures 1-7

Figure S1, related to Figure 1

A

MEPNDSTSTAVEEPDSLEVLVKTLDSQTRTFIVGAQMNVKEFKEHIAASVSIPSEKQRLI
YQGRVLQDDKKLQEYNVGGKVIHLVERAPPQTHLPSGASSGTGSASATHGGGSPPGTRGP
GASVHDRNANSYVMVGTFNLPSDGSAVDVHINMEQAPIQSEPRVRLVMAQHMIRDIQTLL
SRMETLPYLQCRGGPQPQHSQPPPQPPAVTPEPVALSSQTSEPVESEAPPREPMEAEEVE
ERAPAQNPELTPGPAPAGPTPAPETNAPNHPSPAEYVEVLQELQRLESRLQPFLQRYYEV
LGAAATTDYNNNHEGREEDQRLINLVGESLRLLGNTFVALSDLRCNLACTPPRHLHVVRP
MSHYTTPMVLQQAAIPIQINVGTTVTMTGNGTRPPPTPNAEAPPPGPGQASSVAPSSTNV
ESSAEGAPPPGPAPPPATSHPRVIRISHQSVEPVVMMHMNIQDSGTQPGGVPSAPTGPLG
PPGHGQTLGQQVPGFPTAPTRVVIARPTPPQARPSHPGGPPVSGTLQGAGLGTNASLAQM
VSGLVGQLLMQPVLVAQGTPGMAPPPAPATASASAGTTNTATTAGPAPGGPAQPPPTPQP
SMADLQFSQLLGNLLGPAGPGAGGSGVASPTITVAMPGVPAFLQGMTDFLQATQTAPPPP
PPPPPPPPAPEQQTMPPPGSPSGGAGSPGGLGLESLSPEFFTSVVQGVLSSLLGSLGARA
GSSESIAAFIQRLSGSSNIFEPGADGALGFFGALLSLLCQNFSMVDVVMLLHGHFQPLQR
LQPQLRSFFHQHYLGGQEPTPSNIRMATHTLITGLEEYVRESFSLVQVQPGVDIIRTNLE
FLQEQFNSIAAHVLHCTDSGFGARLLELCNQGLFECLALNLHCLGGQQMELAAVINGRIR
RMSRGVNPSLVSWLTTMMGLRLQVVLEHMPVGPDAILRYVRRVGDPPQPLPEEPMEVQGA
ERASPEPQRENASPAPGTTAEEAMSRGPPPAPEGGSRDEQDGASAETEPWAAAVPPEWVP
IIQQDIQSQRKVKPQPPLSDAYLSGMPAKRRKTMQGEGPQLLLSEAVSRAAKAAGARPLT
SPESLSRDLEAPEVQESYRQQLRSDIQKRLQEDPNYSPQRFPNAQRAFADDP

B

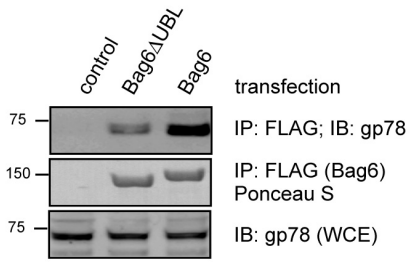

C

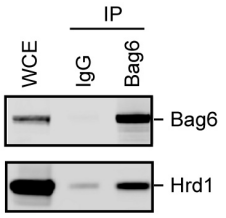

D

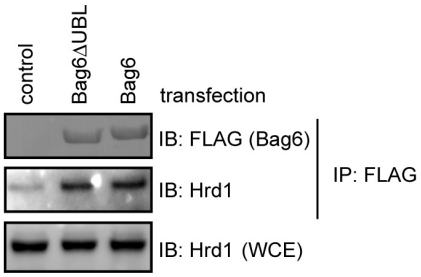

Figure S2, related to Figure 2

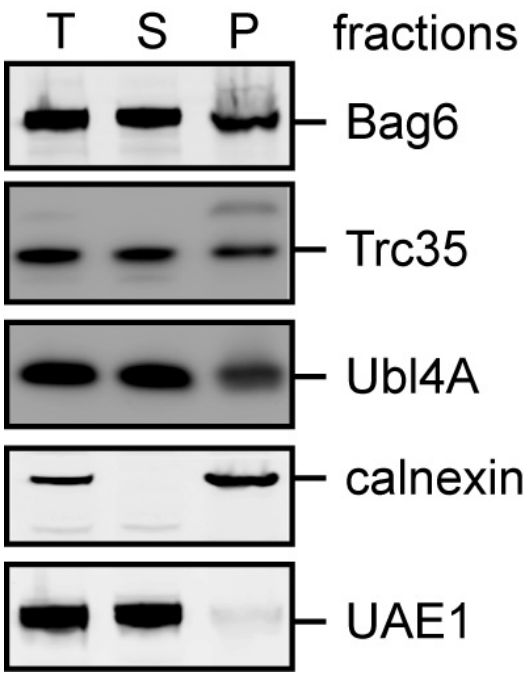

Figure S3, related to Figure 3

A

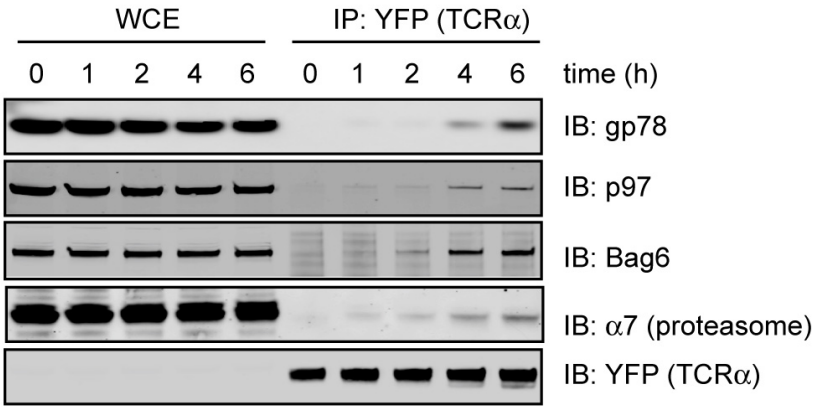

B

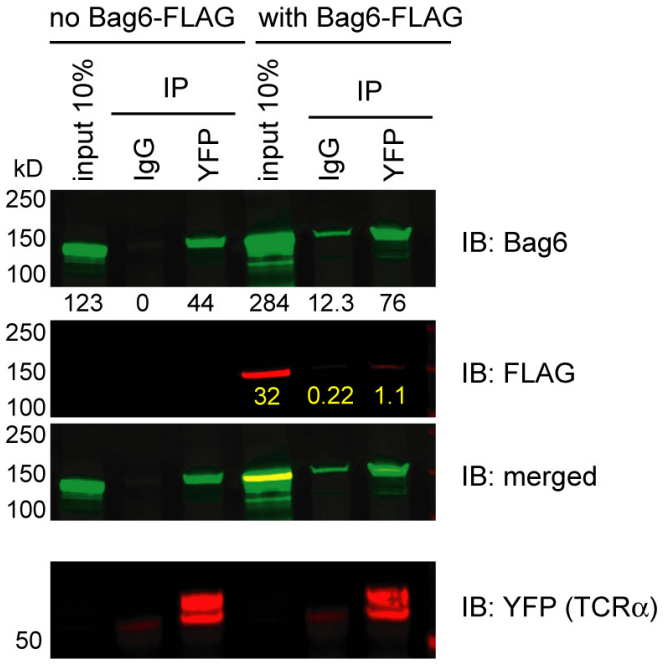

Figure S4, related Figure 4

A

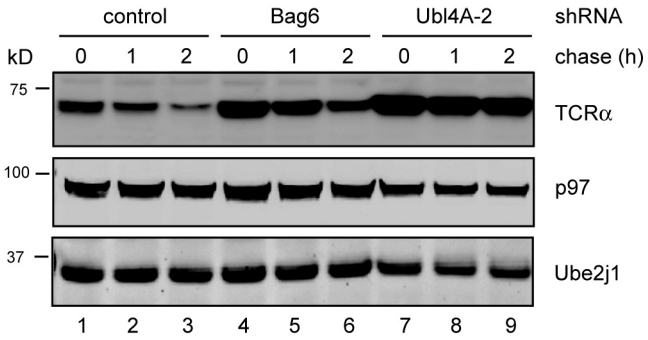

B

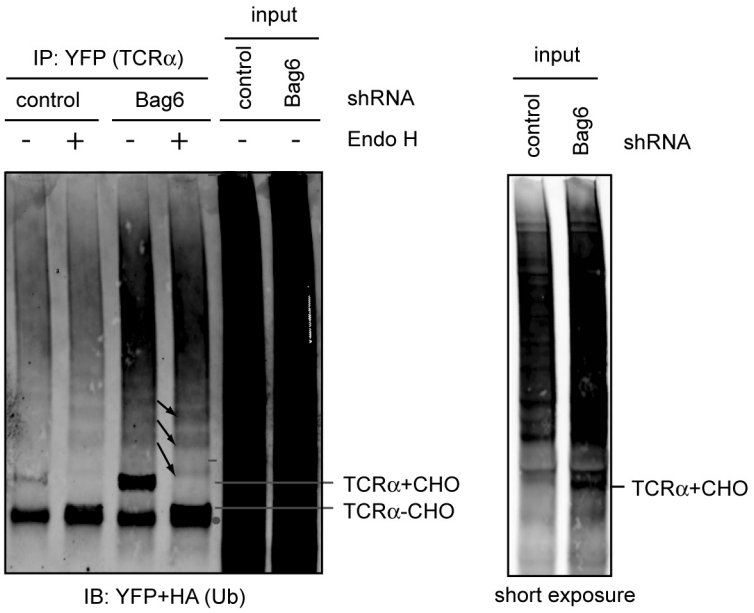

Figure S5, related to Figure 5

A

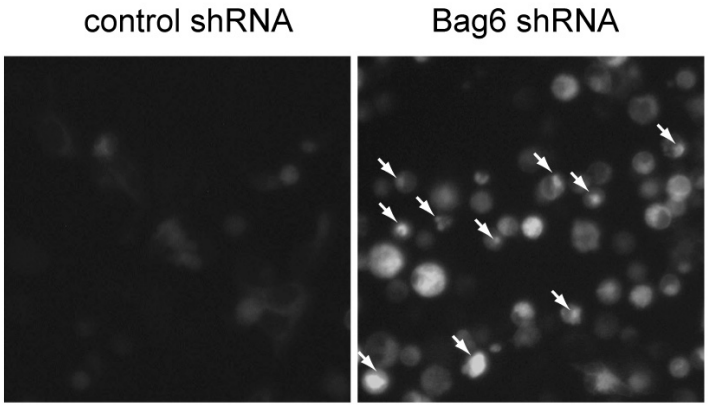

B

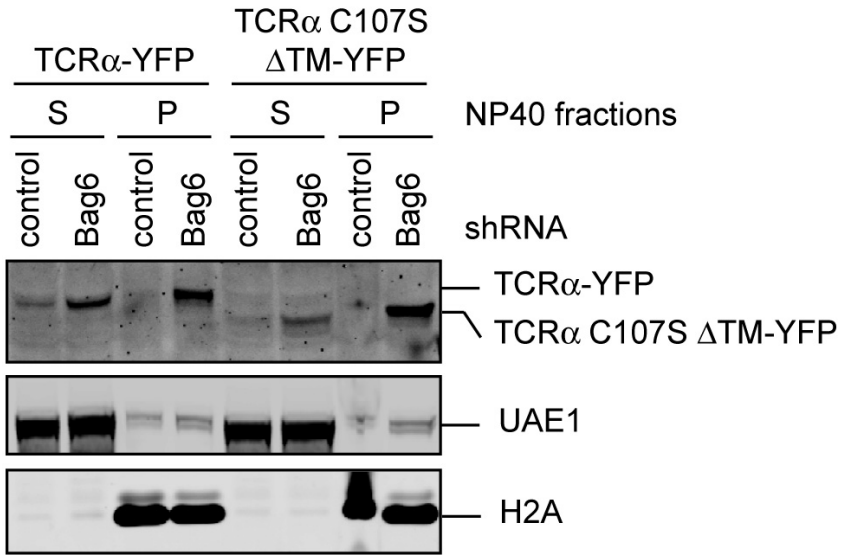

Figure S6, related to Figure 6

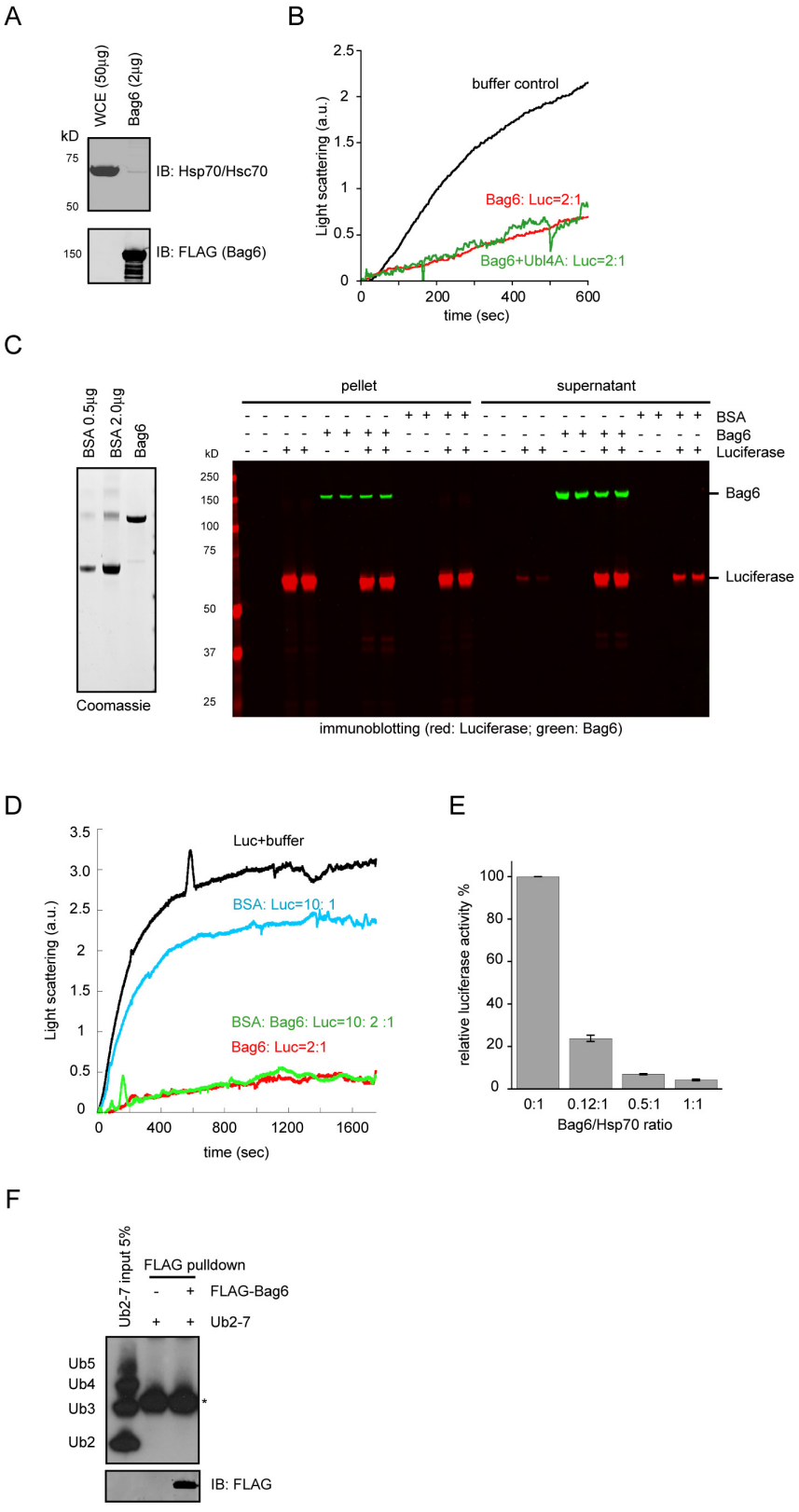

Figure S7, related to Figure 7

A

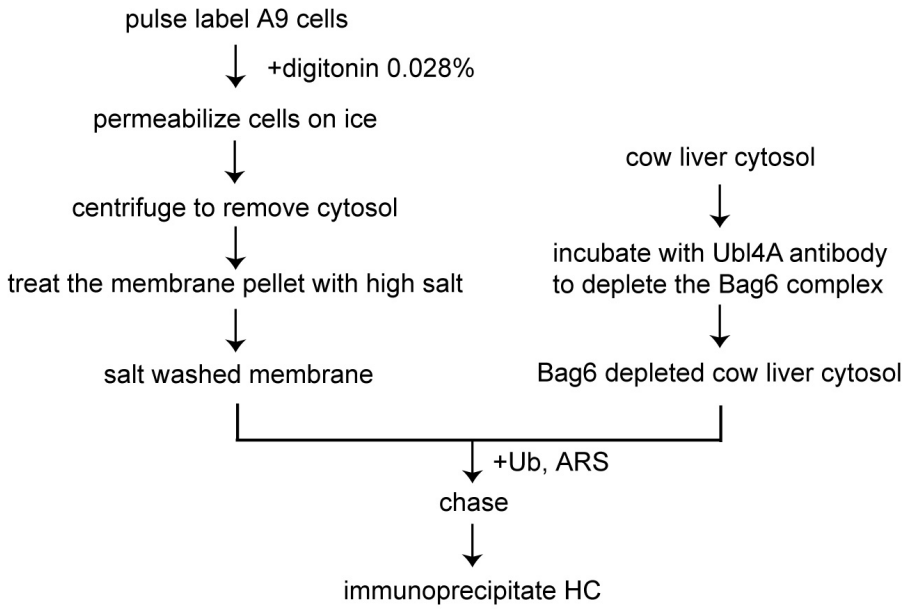

B

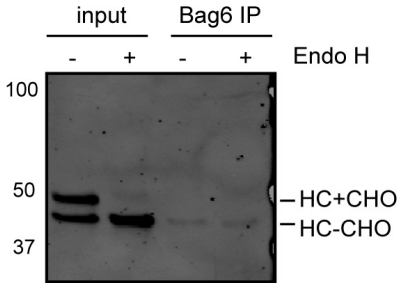

Supplemental Figure Legends

Figure S1, related to Figure 1 Characterization of the interaction of Bag6 with ERAD specific ligases

A, Identification of Bag6 as a gp78-interacting protein. Shown is the amino acid sequence of Bag6. Peptides identified by mass spectrometry are shown in red and blue. **B,** The interaction of Bag6 with gp78 is dependent on the UBL domain. Cell extracts from 293T cells expressing the indicated Bag6 variants were subject to IP with FLAG antibody. **C, D,** Bag6 interacts with the ERAD specific ubiquitin ligase Hrd1. **C,** Detergent extract of 293T cells expressing Myc-tagged Hrd1 was subject to immunoprecipitation (IP) with either control IgG or Bag6 antibody. Endogenous Bag6 interaction with Hrd1-Myc was demonstrated by immunoblotting (IB) with antibodies against the indicated proteins. A fraction of the whole cell extract (WCE) was directly analyzed by immunoblotting. **D,** Detergent extracts of 293T cells transfected with the indicated plasmids were subject to immunoprecipitation with a FLAG antibody and immunoblotting with the indicated antibodies.

Figure S2, related to Figure 2 The Bag6 complex is localized in both cytosol and membrane-associated fractions

293T cells were lysed in a hypotonic buffer. The post nuclear supernatant fraction was either analyzed directly by immunoblotting (T) or first fractionated into a membrane pellet (P) and a cytosolic supernatant fraction before immunoblotting analysis with antibodies against the indicated proteins. Note that the membrane pellet samples were concentrated by 4-fold.

Figure S3, related to Figure 3 Bag6 interacts with the retrotranslocation substrate TCRα in cells

A, Interactions of ERAD machinery proteins with the retrotranslocation substrate TCRα. 293T cells expressing YFP-tagged TCRα were treated with MG132 (20 M) for the indicated time periods. TCRα-YFP-containing complexes were immunoprecipitated from cell extracts prepared with the NP40 lysis buffer. The immunoprecipitated materials were subject to immunoblotting (IB) with the indicated antibodies. Where indicated, a fraction of the whole cell extracts (WCE) were analyzed directly by immunoblotting. **B,** The interaction of Bag6 with TCRα occurs in cells. 293T cells expressing YFP-tagged TCRα were treated with MG132 (10 M) for 12h. Cell extracts were divided into two equal portions. Purified Bag6-FLAG was added to one sample at

a concentration similar to that of the endogenous Bag6. TCRα immunoprecipitated from these samples were analyzed by immunoblotting with the indicated antibodies. The number shows the fluorescence intensity of the indicated bands. Note that the recombinant Bag6 co-precipitated with TCRα was 10-fold less than endogenous Bag6, suggesting that the interaction of Bag6 with TCRα occurs prior to cell lysis.

Figure S4, related to Figure 4 The Bag6 complex is required for TCRα degradation

A, Knockdown of Bag6 and Ubl4A does not affect the stability of endogenous Ube2j1. TCRα-YFP expressing 293T cells treated with the indicated shRNA constructs were subject to cycloheximide chase analysis. Whole cell extracts prepared in the NP40 lysis buffer were analyzed by immunoblotting with the indicated antibodies. **B,** Polyubiquitinated TCRα in Bag6 knockdown cells contains N-glycan. TCRα-YFP-expressing cells were transfected with either control or a Bag6 shRNA-expressing construct together with a plasmid that expressed HA-tagged ubiquitin. Where indicated, TCRα immunoprecipitated under a denaturing condition was treated with Endo H. The arrows indicate mobility shift for oligo-ubiquitinated TCRα after Endo H treatment. The change in mobility is not obvious for TCRα that contains longer ubiquitin chains due to high molecular weight. The dot indicates an IgG band that overlaps with deglycosylated HC.

Figure S5, related to Figure 5 Bag6 maintains the solubility of ERAD substrates

A, Knockdown of Bag6 causes accumulation of TCRα in aggregation-like structures. 293T cells expressing TCRα-YFP together with either control shRNA or Bag6 shRNA were imaged by a fluorescence microscope using the same exposure time. Note that the TCRα-YFP level was significantly higher in Bag6 knockdown cells than in control cells. The arrows indicate TCRα-YFP-containing speckles likely caused by protein aggregation. **B,** Bag6 knockdown causes both TCRα and a TCRα variant lacking TMD to accumulate in the NP40 insoluble state. 293T cells expressing either TCRα-YFP or TCRα C107S ΔTM-YFP together with the indicated shRNA were lysed in the NP40 lysis buffer (S). The NP40 insoluble pellet fractions (P) were extracted with the Laemmli buffer. Both fractions were analyzed by immunoblotting with the indicated antibodies. Note that Bag6 knockdown has a similar effect on the solubility of TCRα regardless of whether it carries a TMD.

Figure S6, related to Figure 6 Bag6 contains a chaperone holdase activity

A, The purified Bag6 sample does not contain significant amount of Hsp70/Hsc70. Purified Bag6 (2μg) was analyzed in parallel with 50μg of 293T cell extract by immunoblotting with the indicated antibodies. **B,** Ubl4A is not required for the holdase activity of Bag6 *in vitro*. Luciferase was incubated with either buffer, Bag6 or a purified Bag6-Ubl4A subcomplex at the indicated molar ratio at 42 ºC. The scattered light was measured by a spectrometer. **C,** The left panel shows a Coomassie blue-stained gel for quantification of the Bag6 concentration. Known amount of BSA was loaded as a reference. The right panel shows a luciferase aggregation experiment similar to the one in Fig. 6C. Luciferase (150nM) was incubated with either buffer, BSA (300nM) or Bag6 (300nM) at 42 ºC for 20min. Luciferase aggregates were sedimented by centrifugation. The pellet and supernatant fractions were analyzed by immunoblotting. The reactions were all performed in duplicates. Note that the presence of Bag6 caused a large amount of luciferase to remain in the soluble fraction. The lack of significant reduction of Bag6 in the corresponding pellet samples was either because the strong immunoblotting signals were out of the detection dynamic range or due to incomplete solubilization of the proteins in the aggregated fractions. **D,** Luciferase (200nM) was incubated with either buffer or the indicated amount of purified Bag6 or BSA at 42 ºC. **E,** Bag6 effectively competes with Hsp70 for binding to luciferase. Luciferase was incubated with a Hsp70 chaperone mixture containing Hsp70 (150nM), HOP (200nM), Hdj1 (300nM) and ATP 5mM in the presence of the indicated amount of Bag6 at 42 ºC for 20min. The error bars show the averaged luciferase activity from two independent experiments. The activity of luciferase in the absence of Bag6 was set as 100%. **F,** Bag6 does not bind ubiquitin directly. Bag6-FLAG immobilized on FLAG agarose was incubated with mixed ubiquitin chains containing 2-7 ubiquitin moieties. The precipitated material was analyzed by immunoblotting.

Figure S7, related to Figure 7 Bag6 is involved in US11-induced ERAD of HC

A, An experiment scheme for the permeabilized cell assay. **B,** Bag6 binds deglycosylated HC. Samples from the experiment shown in Fig. 7F (lanes 1 and 4) were treated with Endo H or mock treated before immunoblotting analysis.

Supplemental Experimental Procedures

Cell lines, chemicals, plasmids, and antibodies

The 293T cell line stably expressing TCRα-YFP was described previously (Wang et al., 2008). Plasmids expressing FLAG-tagged Ubl4A and Trc35 were purchased from Origene (Rockville, MD). The pcDNA-Bag6ΔUBL-FLAG was made by cloning a DNA fragment encoding residues 88 to 1126 of Bag6 to the EcoRV and NotI sites in the pcDNA5/FRT/TO vector (Invitrogen, Carlsbad, CA). For the shRNA experiments, the targeting sequences are:
Bag6 shRNA: ACCGGAATGCCAACAGCTATGTCATGGTT
Trc35 shRNA: CTGTGCCAACATGCTGGTGGAGTATTCCA
Ubl4A shRNA-1: GCCATGTATATGGCTTCAA
Ubl4A shRNA-2: GATGAACATATCCCAGCCAA

TransIT®-293 (Mirus) was used for plasmid transfection, and lipofectamine2000 (Invitrogen) was used for experiments involving gene knockdown. Antibodies to Bag6, Ubl4A, Trc35, gp78, Ube2g2, GFP were described previously (Li et al., 2009; Mariappan et al., 2010). Other antibodies used are FLAG (M2) (Sigma), p97 (Fitzgerald), UAE1 (Sigma), UbxD8 (Proteintech Group), Histone H2A (Abcam), ubiquitin (Santa cruz), and MMS1 (BIOMOL). MG132 was purchased from EMD Bioscience. Luciferase was purchased from Sigma. Hsp70, Hdj1, HOP were purchased from ENZO life sciences. Ub2-7 was purchased from Bostonbiochem.

Immunoblotting and immunoprecipitation

Cells were lysed in the NP40 lysis buffer containing 50mM Tris-HCl pH 7.4, 150mM sodium chloride, 2mM magnesium chloride, 0.5% NP40, and a protease inhibitor cocktail, or a RIPA buffer containing 50mM Tris pH 7.5, 1% NP40, 0.1% SDS, 0.5% sodium deoxycholate, 150mM sodium chloride, 2mM EDTA. Cell extracts were subject to centrifugation to remove insoluble materials. For most experiments, the supernatant fractions were analyzed. Where indicated, the NP40 insoluble pellet was resolubilized either by the Laemmli buffer for immunoblotting, or by 1% SDS and 5mM DTT for immunoprecipitation in the pulse chase experiments. The solubilized materials were diluted with the NP40 lysis buffer so the final extract contained 0.1% SDS and 0.5mM DTT before immunoprecipitation analyses. Immunoblotting was performed according to the standard protocol. Fluorescence-labeled secondary antibodies (Rockland) were used for detection. The fluorescent bands were imaged and quantified on a *LI-COR* Odyssey infrared imager using the software provided by the manufacture. For immunoprecipitation under denaturing condition, cells were lysed in a buffer containing 1% SDS 5mM DTT. Cell extracts

were heated at 65 ºC for 15min and subsequently diluted 10-fold with the NP40 lysis buffer. Soluble materials were used for immunoprecipitation.

Immunostaining and flow cytometry

For flow cytometry experiments, cells were resuspended in a phosphor saline buffer and analyzed in a Cytomics FC 500 (BeckmanCoulter). For immunofluorescence microscopy studies, cells growing on cover slips or in Lab-Tek slide chambers (Nalge Nunc International, Rochester, NY) were fixed in the phosphor saline solution (PBS) containing 4% paraformaldehyde. Cells were permeabilized in a solution containing 0.1% NP40 and 4% fetal bovine serum and stained with primary and secondary antibodies in the same buffer. Cells were counterstained with a mounting medium containing DAPI to illuminate the nucleus. Images were taken with an Axiovert 200 inverted microscope equipped with a 63X oil immersion Plan-Apochromat objective (N/A 1.4). Confocal microscope analyses were performed with a Zeiss LSM 780 system.

Protein purification

To purified Bag6 variants or the Bag6-Ubl4A subcomplex, 293T cells were transfected with the corresponding expression plasmids. Cells were harvested 72 hours post transfection in a buffer containing 1% DeoxyBigCHAP, 30mM Tris/HCl pH 7.4, 150mM potassium acetate, 4mM magnesium acetate and a protease inhibitor cocktail. The cleared cell extract was incubated with FLAG-agarose beads (Sigma) and the bound materials were extensively washed with a buffer containing 1% DeoxyBigCHAP, 30mM Tris/HCl pH 7.4, 500mM potassium acetate, 4mM magnesium acetate. The bound materials were eluted using 0.2mg/ml 3 X FLAG peptide (Sigma) in 25mM Hepes, pH 7.2, 115mM potassium acetate, 5mM sodium acetate, 2.5mM magnesium acetate.

In vitro permeabilized cell assay

Pulse chase and permeabilization experiments were performed as follows. U373-MG astrocytoma cells stably expressing US11 and the HA tagged MHC class I heavy chain HLA-A2 (HC) were starved in a Met/Cys free DMEM medium for 40 min and then incubated in a medium containing ^{35}S-Met/Cys for 10 min to label nascent HC. To permeabilize the plasma membrane,

cells were washed with PBS supplemented with 0.9mM $CaCl_2$ and then incubated at $3X10^7$ cells/ml in the PB buffer (25mM Hepes, pH 7.2, 115mM potassium acetate, 5mM sodium acetate, 2.5mM MgCl2, 0.5mM EGTA) containing 0.028% digitonin (Calbiochem, Gibbstown, NH) and a protease inhibitor cocktail at 4 ºC for 5min. Permeabilization efficiency was confirmed by staining cells with the Trypan blue dye. Cells were subject to centrifugation at 20,000g to remove cytosol. The membrane pellet fraction was further washed with a PB buffer containing 250mM NaCl. Salt washed membrane was then incubated with 3000μg mock depleted or Bag6-depleted cow liver cytosol in the presence of 10μM bovine ubiquitin and an ATP regenerating system (ARS). The reaction was incubated at 37 ºC. Samples taken at different time points were solubilized in the NP40 lysis buffer and analyzed by immunoprecipitation with an anti-HA antibody.

Supplemental References

Li, W., Tu, D., Li, L., Wollert, T., Ghirlando, R., Brunger, A. T., and Ye, Y. (2009). Mechanistic insights into active site-associated polyubiquitination by the ubiquitin-conjugating enzyme Ube2g2. Proc Natl Acad Sci U S A *106*, 3722-3727.

Mariappan, M., Li, X., Stefanovic, S., Sharma, A., Mateja, A., Keenan, R. J., and Hegde, R. S. (2010). A ribosome-associating factor chaperones tail-anchored membrane proteins. Nature *466*, 1120-1124.

Wang, Q., Li, L., and Ye, Y. (2008). Inhibition of p97-dependent protein degradation by Eeyarestatin I. J Biol Chem.